Czech Technical University in Prague
Faculty of of Electrical Engineering
Department of Measurement

Virtual Sensors for Data Validation and Performance Monitoring

by

Ing. Vladimír HORYNA

Doctoral Thesis

Supervisor: Prof. Ing. Radislav ŠMÍD, Ph.D.
PhD programme: Electrical Engineering and Information Technology (P2612)
Branch of study: Measurement and Instrumentation (2601V006)

Prague, October 2019

Supervisor:
Prof. Ing. Radislav ŠMÍD, Ph.D.
Department of Measurement
Faculty of Electrical Engineering
Czech Technical University in Prague
Technická 2
166 27 Prague 6
Czech Republic

Abstract

- Title: Virtual Sensors for Data Validation and Performance Monitoring
- Author: Ing. Vladimír Horyna
- Department: Department of Measurement, CTU in Prague, FEE
- Supervisor: Prof. Ing. Radislav Šmíd, Ph.D., Department of Measurement

Power saving is one of the main topics of buildings management. In commercial buildings, the HVAC (Heating, Ventilation, and Air Conditioning) system is one of the largest energy consumers. The energy savings in the HVAC systems can be achieved by novel methods of fault detection and diagnostics (FDD) and performance monitoring. In practical application, the first challenge is the absence of the sensors needed to diagnose the HVAC systems; the second issue is the difficult configuration of the methods for a specific use.

This work presents the possible solution using Virtual Sensors (VS) and automatic configuration. VS represent a low-cost alternative for missing real sensors, for the automatic FDD configuration the use of Building Information Model (BIM) is introduced. The information needed to configure the VS automatically is obtained from BIM using IFC ontology.

This work presents two kinds of virtual sensors: The Virtual Mass Flow Sensors for an Air Handling Unit (AHU) and virtual sensor of zone temperature. Laboratory experiments have confirmed that the proposed Virtual Mass Flow Sensors can be utilized as a substitute for a physical mass flow rate sensor for monitoring and fault detection. The virtual sensor of zone temperature was tested in a real building, and the results confirmed that this VS could be used to data validation of the real temperature sensor.

Keywords:

Virtual Sensors, HVAC system, The Building Information Model, BIM, Industry Foundation Classes release 4, IFC4, Ontology, AHU unit, Fault Detection and Diagnostics, FDD, Performance Monitoring.

Abstrakt

- Název práce: Virtuální sensory pro validaci dat a monitorování
- Autor: Ing. Vladimír Horyna
- Katedra: Katedra měření, ČVUT v Praze, FEL
- Vedoucí disertačí práce: Prof. Ing. Radislav Šmíd, Ph.D., Katedra měření

Úspora energie je jedním z hlavních témat v oboru řízení a diagnostiky budov. Jedním z největších spotřebitelů energie v komerčních budovách je HVAC systém (Heating, Ventilation and Air Conditioning). Úspory energie v systémech HVAC, lze dosáhnout novými metodami detekce a diagnostiky poruch (FDD) a sledováním výkonu těchto systémů. V praktické aplikaci nových FDD se setkáváme se dvěma zásadními problémy. První výzvou je absence senzorů potřebných k diagnostice systémů HVAC. Druhým problémem je obtížná konfigurace FDD metod pro konkrétní použití.

Tato práce představuje virtuální senzory (VS) s automatickou konfigurací jako jedno z možných řešení tohoto problému. VS představují levnou alternativu pro chybějící skutečné senzory, pro automatickou konfiguraci FDD je použit informační model budovy (Building Information Model BIM). Informace potřebné pro automatickou konfiguraci VS jsou získány z BIM pomocí IFC ontologie.

Dva druhy virtuálních senzorů jsou publikovány v této práci: Virtuální senzory hmotnostního průtoku vzduchu pro vzduchotechnickou jednotku (AHU) a virtuální senzor teploty unitř místnosti (obecně zóny). Laboratorní experimenty potvrdily, že navrhované virtuální senzory hmotnostního průtoku vzduchu mohou být použity jako náhrada za skutečný senzor hmotnostního průtoku vzduchu v FDD systémech. Virtuální senzor teploty zóny byl testován v reálné budově a výsledky potvrdily, že tento VS lze použít k ověření dat skutečného teplotního senzoru.

Klíčová slova:

Virtuální seznory, HVAC ststém, Informační model budovy, BIM, IFC4, Ontologie, AHU jednotka, Detekce a diagnostika poruch, FDD, Sledování výkonnosti zařízení.

Acknowledgment

First of all and foremost, I have to thank my family for their love and great support.

I want to give my sincere thanks to my supervisor, Prof. Radislav Šmíd, PhD., for his guidance and support throughout my studies.

I declare that I carried out this doctoral thesis independently, and only with the cited sources, literature and other professional sources.

In Prague date . . . . . signature of the author

Contents

List of Figures

List of Tables

Chapter 1

Introduction

1.1 Motivation

Power saving is becoming one of the main topics of buildings control. The strongest driving force is the increase in energy prices. Therefore the reduction of energy consumption is needed. The second is the fact that buildings consume 20% to 40% of the total world energy consumption [1]. A significant energy consumer in commercial buildings is the HVAC (Heating, Ventilation, and Air Conditioning) system. HVAC systems consume 40% to 50% of building energy consumption [2]. Up to one half of the energy used in HVAC systems are needless expenditures[3]. These needless expenditures are caused by poorly maintained, degraded, and improperly controlled HVAC systems.

Energy savings can be achieved at minimal cost by improving building automation systems, e.g., by implementing performance monitoring [4, 5], by improving HVAC control system performance [6, 7] and by applying Fault Detection and Diagnostics (FDD) in the HVAC system. From an HVAC point of view, this can be summarized as follows:

- Improved HVAC control.
- Early detection and elimination of HVAC system faults.
- Performance monitoring and timely maintenance of HVAC.
- Energy usage forecasting and economical use of resources (e.g. exhaust-heat storage).

The **Performance Monitoring** and **Fault Detection and Diagnostics** (**FDD**) are specialized areas of observing of the HVAC system. Performance monitoring is aimed at notifying the user about possible problems causing energy waste. FDD methods are aimed at identification and finding the cause of faults. There are many methods of performance monitoring and FDD [3, 8]. Practical application of these methods is subject to two significant technical challenges:

- **Missing sensors** (i.e. HVAC systems contain only a basic set of sensors designated for control, not for performance monitoring). The **Virtual Sensors (VS)** can be the solution to this problem.
- **The missing or inadequate information** about HVAC system (e.g. exact hardware configuration is absent, the problem is closely involved with the high variability of HVAC systems and HVAC control configuration). **The Building Information Model (BIM)** can be a solution to this problem.

Yu et al. wrote an overall review of FDD methodologies that are available for Air Handling Units (AHU) [9]. Due to cost constraints, most of the methods that have been published are based solely on temperature measurements, set-point values, and control signals [9, 3]. The performance of these FDD methods is therefore limited by the reduced amount of information about process variables. **Virtual sensing techniques** can solve this problem. Virtual sensing techniques enable the development of cost-effective and robust FDD systems [10, 11] for commercial buildings, with reported savings of up to 50% for energy costs and up to 70% for service costs. **Virtual Sensors** estimate the desired quantity using available physical sensors and mathematical models. Typically when it would be expensive to measure a particular quantity, or when it would be physically challenging to provide measurements [12]. The technical problem that prevents extensive practical use of VS is their typical demanding configuration for a specific application. However, this process can be fully or partially automated, and input information about a specific VS application can be B**uildings Information Model**. VS are not only a cheaper alternative to physical sensors. In some cases, they can even provide more reliable and more accurate measurements (mixed air temperature in AHU, air flows, etc.) [10].

1.2 Problem Statement

Performance monitoring and FDD methods require input information to function correctly. Data from sensors (and history of measurement) are the essential inputs. Sensors suited for FDD and performance monitoring are missing in HVAC systems very often [13, 14]. This fact poses a problem for FDD. Deployment of additional sensors required by FDD methods is a frequent problem, mainly in economic terms. **Virtual Sensors** represent a low-cost alternative for missing real sensors. For simplicity's sake, virtual sensors can be imagined as software, which determines the missing value from other known information [10]. Virtual sensors also enable the use or improve the performance of other HVAC energy optimization tasks, such as improving HVAC control and energy usage forecasting. The proposed dissertation aims at research and development of virtual sensors for the use by an FDD system and performance monitoring.

The following essential input information for FDD methods of HVAC is contextual information about HVAC hardware configuration (building information can be beneficial too).

This contextual information could be used for virtual sensor configuration. Contextual information about HVAC hardware configuration (and building) is challenging to obtain. Manual retrieval of information from the building's documentation is time-consuming, and this method needs a lot of human resources. For automatic retrieval of contextual information, it is possible to use **Building Information Model** (**BIM**) [14, 15]. Building information modeling is the process of capturing and managing building data during its life cycle [16]. BIM can help to get the right information on, e.g., specific sensor placement, or connection between components of the HVAC system. The next goal of the dissertation is this: FDD applications will be able to get a majority of information needed for their setup automatically without human intervention.

The existence of input values itself isn't a sufficient condition for the correct functioning of FDD methods [17]. **Data validation** is indispensable for the accurate workings of FDD methods. Methods for invalid value detection (such as an out-of-range-value detector and an oscillation detector) can use virtual sensors and BIM information as well. The virtual sensor can be added to a real sensor. If the value of the real sensor differs distinctly from the virtual sensor value (awaited, calculated value), the real sensor value will be indicated as a suspect. For these reasons, methods for data validation will be solved in the dissertation too.

Figure 1.1. shows a theoretical block diagram of the HVAC performance monitoring system. The performance monitoring system uses all three of the methods mentioned above (Virtual sensors, BIM contextual information, and Data validation). Imagine this hypothetical situation: an HVAC system includes set of real sensors: Air temperature in all zones (rooms), Supply air at the inlet of the recuperator, Supply air at the outlet of the recuperator, Exhaust air at the inlet of the recuperator, and Exhaust air at the outlet of the recuperator. For performance monitoring the verification of the zone air temperature is needed as well as an estimation of the mass flow rate through the HVAC system.

Virtual sensor 1 calculates air temperature in the zone based on temperatures in the adjacent zones and context information from the BIM about building construction. This value is used for data validation of the real temperature sensor in the zone. Virtual sensor 2 estimates the mass flow rate through the HVAC system. Virtual sensor 2 uses temperature data around the recuperator and recuperator's parameters from the BIM.

Thanks to the performance monitoring system, needless expenditures on heating and air conditioning can be detected. Based on data validation of zone temperature, open window, or drift of output value from the real temperature sensor can be revealed. The drift of output value from the temperature sensor can also cause loss of comfort in the zone. Based on the calculated airflow rate in the HVAC system (VS 2), for example, a stuck of the outer air damper or filter clogging can be detected. Increased air heating costs can be caused by the stuck of the outer air damper.

Based on this example, a possible use of virtual sensors and building information models

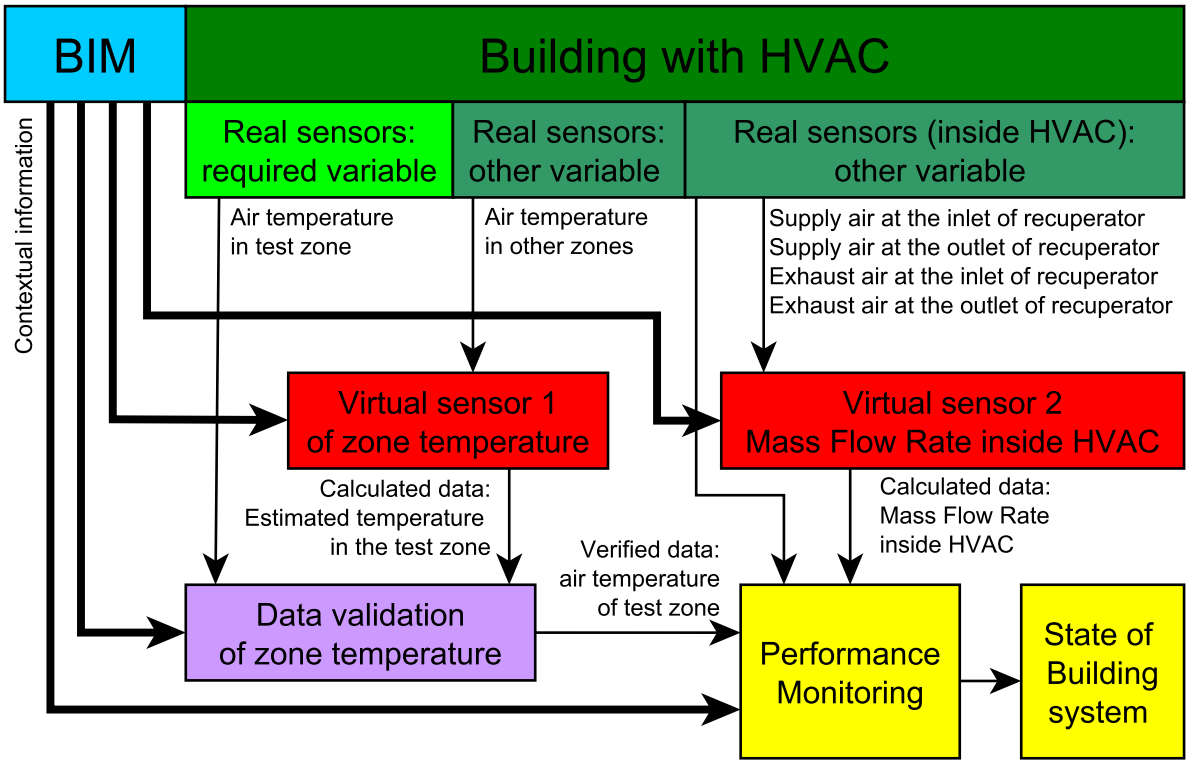

Figure 1.1: Example FDD with virtual sensors and BIM.

for data validation and performance monitoring of the HVAC was described. Both virtual sensors from this example are developed and described in this work.

Chapter 2

Background and State-of-the-Art

2.1 Virtual Sensors

This chapter gives an overview of the principles and ideas in virtual sensors (VS) used for monitoring and fault detection. Methods in this section will be concentrated primarily on virtual sensing technology in buildings.

Virtual sensors have found widespread application in control engineering processes since the early 1980s [19]. An extensive review of virtual sensors was published by Li at al. [10]. A basic definition is formulated by Fortuna et al.: *"Soft sensors focus on the process of estimation of any system variable or product quality by using mathematical models, substituting some physical sensors and using data acquired from some variables one"* [20]. Many publications used **soft sensors** [20, 21], but in this paper will virtual sensor be used.

Virtual sensors have found widespread application ranging from automotive [10] (knock detection [22]), avionics (SHM [23]), building monitoring [10] to fault detection for machine tools [24]. The primary objective of the virtual sensor is to address the challenge of missing data from the real sensor. Virtual sensors represent a low-cost (or no-cost) solution to missing real sensors, since they eliminate the necessity of purchasing and installation of the missing sensors. Virtual sensors can be divided into two groups of topology. Local virtual sensor and distributed virtual sensors (the computation is distributed between spatially distributed units, typically nodes in wireless). Virtual sensors are replacement for physical sensors in various situations:

- A physical sensor is costly, difficult to install or maintain.
- No room to put in the physical sensor.
- Measurements provided by physical sensor are too slow.

- A physical sensor is too far downstream from the application point of view (unusable for control).
- Estimated quantity is unavailable for sensing.

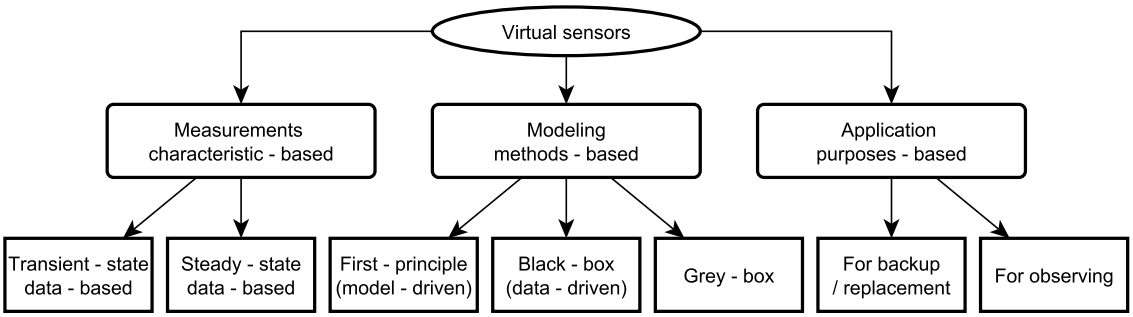

Figure 2.1: Categorization scheme for virtual sensors [10].

Figure 2.1. shows categorization scheme for virtual sensors. On the basis of measurement characteristics of two kinds of virtual sensors are distinguished:

- **Transient response (indicial response):** contains a transient model to predict the transient behavior, e.g. for feedback control.
- **Steady-state variables:** the modeled process is quasi-static, e.g. for performance monitoring or fault identification.

The principle of modeling methods-based an virtual sensors can be described as a functional mapping from a multi-dimensional input to one/multi-dimensional output, fusing the information of various sensor sources. The extraction of the desired relationship is a crucial task and the following approaches are used:

- **First principle approach** or **A white box approach** (model-driven): the virtual sensor is derived from fundamental physical laws and have parameters with physical significance.
- **Black box approach** (data-driven): design of virtual sensor utilize empirical correlations without any knowledge of the physical relationships. Statistical tools such as Principal Component Analysis (PCA), Support Vector Regression (SVR), the Proportional Integral Observer (PIO), and Neural Networks are typically used.

- **Grey box approach** (hybrid approach): design is based on a combination of physical and empirical models for estimating the output of an unmeasured process.

Safety-critical systems is important application of virtual sensors, where redundancy of measurements is used to detect physical sensor failure [25]. Virtual sensors can also provide indirect measurements of abstract conditions (that, by themselves, are not physically measurable) by combining sensed data from a group of heterogeneous physical sensors. Virtual sensors can be categorized according to application:

- **Secondary (backup) sensor:** used for fault detection of existing physical sensors or as redundant sensor for backup of existing physical sensors.
- **Primary sensor (observer):** used individualy for the measurement of physical quantity not measured by any physical sensor.

Although developing (or function) of virtual sensors is the domain-specific process, generally, it can be divided into three phases: data collection, signal (pre)processing and mapping input information to output value [10, 24]. Proper data collection and preprocessing strongly affects accuracy and reliability of virtual sensors. Data verification and validation is notorious issue of FDD (Fault Detection and Diagnostics) [13, 14, 25]. We can not expect good results of virtual sensor (generally of FDD), if we do not provide verified input data. In my work I would like to extend the virtual sensors concept of contextual information about current input data. Typical arrangement of virtual sensor with contextual information is displayed in figure 2.2.

2.1.1 First principle approach

The first principle model is one that uses the computation of a quantity, starting directly from laws of physics without making assumptions such as empirical relations or fitted relations. If a first principle model describes the relations between measured and computed quantities sufficiently accurately, a model-based sensor can be derived.

The standard method to design a virtual sensor is usually a two step procedure: in the first step a model is built from first principle. Then, an optimal estimator in a minimum variance sense is designed for the model. The model accuracy is critical for success of virtual sensor development.

The typical first principle virtual sensor was used by Ward and Siegel [26]. Their papers were concerned with virtual filter efficiency sensor. The proposed idea was to apply the measured pressure drop of the filter to determine the airflow through the bypass

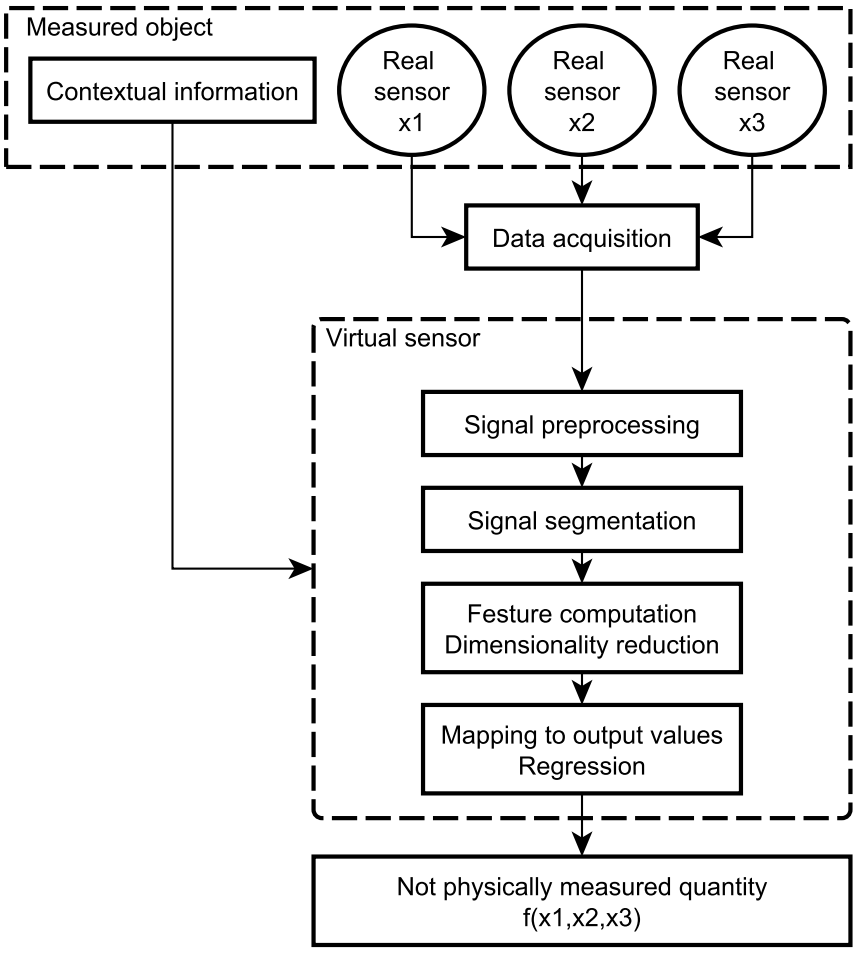

Figure 2.2: Typical virtual sensor block scheme.

cracks. This will account for particle loss through the bypass cracks. The results showed how important it is to monitor the efficiency of the filter, because continuously increasing scarcely visible gaps can have a dramatic effect on the performance of the filters.

Jin et al. [27] used a first principle approach for a dynamic cooling coil unit model. The model was derived based on heat transfer principles and mass and energy balances. Li and Braun presented series of papers which are focused on sensors for vapor compression air-conditioners [28]. Eleven virtual sensors were developed and validated for the principal components of the vapor compression system: the compressor, the condenser, and the expansion valve. The proposed VS (Virtual Sensors) utilizes steady state measurements from four temperature sensors mounted on the surface. Reported charge predictions were within 8% of the actual charge.

An array of first principle models of basic HVAC (Heating, Ventilation, and Air Conditioning) components was arranged Tashtoush at al. [29]. The basic description of HVAC components is possible to find in the handbook ASHRAE [30]. There is a lot of information suitable for first principle virtual sensors for the use of HVAC systems. A lot of first principle (or grey box) models of the building heat dynamics exist (e.g. [31, 32]). I use these heat models to estimate the room temperature.

Yu et al. presented a virtual sensor of the supply air flow rate [60]. The method uses a first-principle model in combination with virtual temperature sensors. Two approaches were proposed: a cooling mode-based method, and a heating mode-based method. It was concluded that the heating-based method is more reliable and more robust than the cooling-based approach.

2.1.2 Black box approach

Black-box (data-driven) approaches utilize empirical correlations without any knowledge of the physical process [3]. There are a number of statistical tools that can be used by black-box virtual sensors. For example Principle Component Analysis (PCA) [10], Support vector machine (Support Vector Regression) (SVR) [22, 21, 33], Proportional Integral Observer (PIO) [23], Neural Network [25] and other.

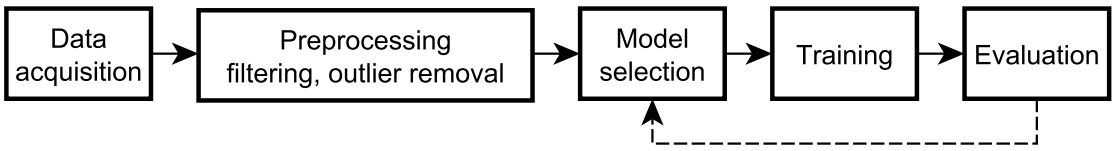

Figure 2.3: Design steps for data-driven virtual sensor.

The principle of black-box virtual sensors is displayed in figure 2.3. In implementation of the data-driven virtual sensors, the training set contains elements which consist of paired variables of the independent input variable and the dependent output variable, which needs to be estimated. The test set contains similar pairs and it is used for performance evaluation and to cope with over- and under-fitting problems. The overfitting occurs when a model describes noise instead of the underlying relationship f(x1,x2,...), the underfitting means increasing of errors due to too simple model of relationship (e.g. linear fit used for quadratic relationship).

The success of data-driven virtual sensor design is often limited by *the curse of dimensionality* (also known as the Hughes effect). With a fixed number of training samples, the

predictive power reduces as the dimensionality increases. For large number of real physical quantities, the performance of the data-driven virtual sensor is unsaticfactory due to sparse sampling of the quantities of space. In order to successfully learn from a finite number of data samples in a high-dimensional feature space, an enormous amount of training data is required. Such a large data sample is needed to ensure that there are several samples with each combination of values.

As an example a virtual sensor of mixed air temperature and the cooling model by Yang and Li can be mentioned [34]. Yang and Li used simple calculations based on the mathematical regression method. Mixed Air Temperature (MAT) is an important parameter for control and FDD for economizers and vapor compression cycles. Damper position signals, the outdoor air temperature, the return air temperature, and a calibrated virtual outdoor air ratio sensor were used as inputs of VS.

The virtual sensors of total cooling capacity proposed by Yang and Li are based on the manufacturer's rating data [10]. The model covers all operating conditions of the cooling system, and the overall tested predictions of the cooling capacity are within 10%.

An approach similar to virtual sensing technology was used by Daihong, Haorong, Long and Yanshun for fault detection of the supply air temperature sensor in rooftop air conditioning units [66]. The outputs of a real sensor were compared with a model, and the results were used to determine the range of proper operating conditions. Cheung and Braun presented an algorithm to minimize the amount of data collection for calibration of virtual sensors [67]. The algorithm is based on the user-specified requirements such as accuracy, reliability and applicability and minimizes the amount of data needed for calibration of a virtual sensor during normal operation of an air conditioning unit.

2.2 Building Information Model

Building Information Modelling (BIM) was defined by The National Building Information Model Standard Project Committee as follows: *"BIM is a digital representation of physical and functional characteristics of a facility. A building information model is a shared knowledge resource for information about a facility forming a reliable basis for decisions during its life-cycle 2.4; defined as existing from earliest conception to demolition"*[35]. BIM connects information about building within the Architecture, Engineering, Construction and Operations industry. Succar [36] worked out a BIM framework through an extensive research. BIM is now being adopted and promoted by building developers, civil engineering organizations and software for architects [14, 37, 38]. An overview of the possible use of BIM and development tools is shown in the figure 2.5. BIM models bring a lot of value also to building automation, BIM can help to get the right information on e.g. specific sensor placement, damper settings, or connection between HVAC entities. [14, 15].

There are many possibilities how to represent a BIM model. BIM **Industry Foundation Classes release 4 (IFC4)** was selected for the proposed dissertation. For more information see section 2.2.1 Ontology.

BIM is possible to be used as an information input for model parametrization. BIM can also provide following information for FDD methods:

- **Contextual information** Additional information of sensor output values or the actual power of heating: e.g.technical specifications of the heater, parameters and position of the sensor, technical specifications of the fan.
- **Input variables:** Input values for calculation of mathematical model: e.g. the size of the room, thickness, the building materials and thermal conductivity of wall, etc.

BIM can provide the information for simulation and models. Many authors use BIM information extraction for building energy simulation [40, 41, 42]. Building energy simulation often requires only a geometric representation of the building as well as data about the objects (wall, window, door, etc.). These specifications are possible to be extracted from BIM. Kota et al. used the geometric information from BIM for simulation of daylight in the room [43]. If a BIM exists, it nearly always includes a geometric representation of the building. The automatic extraction of geometric representation from BIM saves a lot of human labor.

Kim et al. describes BIM information extraction problems [15]. A few limitations of BIM information extraction were observed as well as several problems, namely:

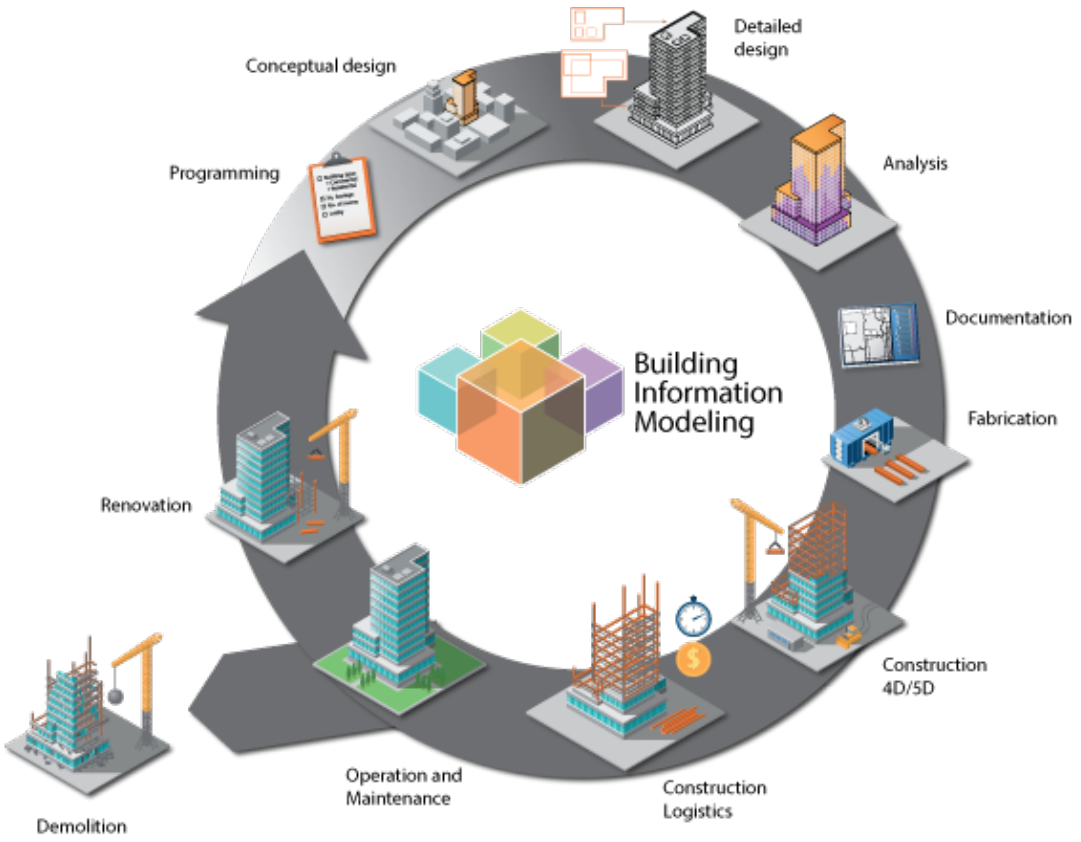

Figure 2.4: BIM life-cycle. (Source: thebimhub.com)

- Multiple representations of the same information complicates the reading of data from BIM.
- Data processing is time-consuming for complicated BIM.
- Absence of BIM from old buildings.
- Underutilized potential of BIM. E.g. in HVAC system a boiler is used, but all technical specifications are missing.
- BIM is incorrect or inaccurate. The BIM was not updated after a previous HVAC renovation.

The above mentioned problems will be removed in the future because many of the big companies are exerting pressure on builders requiring them to have a correct BIM. The

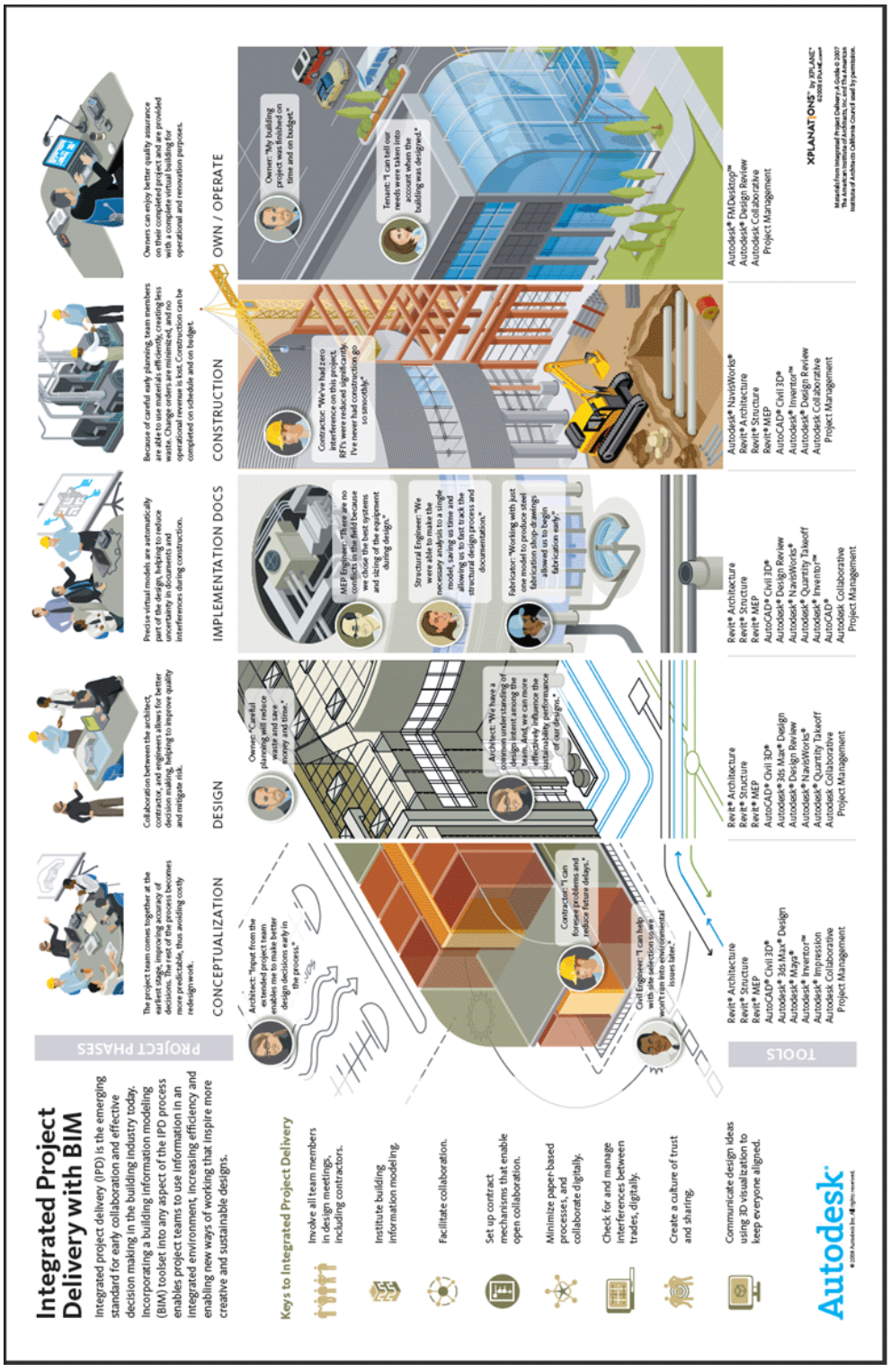

Figure 2.5: Integrated project delivery with BIM. (Source: thebimhub.com)

correct BIM enables substantial improvement to a lot of branches of building engineering (project planning, financial strategies, HVAC control, FDD, ...)[14, 15, 36, 44].

2.2.1 Ontology

The main advantage of BIM is a possibility to exchange and reuse the information over the building life cycle in standardized way using ontology. Ontology is a formal description and definition of the types, properties, and interrelationships of the entities that exist in an application domain.

Definitions of ontology:

- An ontology is a formal naming and definition of the types, properties, and interrelationships of the entities that really or fundamentally exist for a particular domain of discourse.
- A domain ontology (or domain-specific ontology) represents concepts which belong to part of the world. Particular meanings of terms applied to that domain are provided by domain ontology.
- Since domain ontologies represent concepts in very specific and often eclectic ways, they are often incompatible. As systems that rely on domain ontologies expand, they often need to merge domain ontologies into a more general representation. This presents a challenge to the ontology designer. Different ontologies in the same domain arise due to different languages, different intended usage of the ontologies, and different perceptions of the domain
- At present, merging ontologies that are not developed from a common foundation ontology is a largely manual process and therefore time-consuming and expensive. Domain ontologies that use the same foundation ontology to provide a set of basic elements with which to specify the meanings of the domain ontology elements can be merged automatically

BIM IFC specification was selected like ontology for relationship between BIM and virtual sensors. (Specifically the IFC4.2 standart version 4.2.0.0 was selected.) The IFC specification is developed and maintained by buildingSMART International. IFC4 is registered with ISO as ISO16739 [35]. IFC4 was selected because it contains all entities of HVAC system [39], and it is supported by ArchiCAD and Autodesk Revit software. BuildingSMART International publishes official ontology definitions. The documentation is deposited at standards.buildingsmart.org. The data schema architecture of IFC defines four conceptual layers, each individual schema is assigned to exactly one conceptual layer [39]. Figure 2.6 shows the schema architecture.

Definition of individual layers [39]:

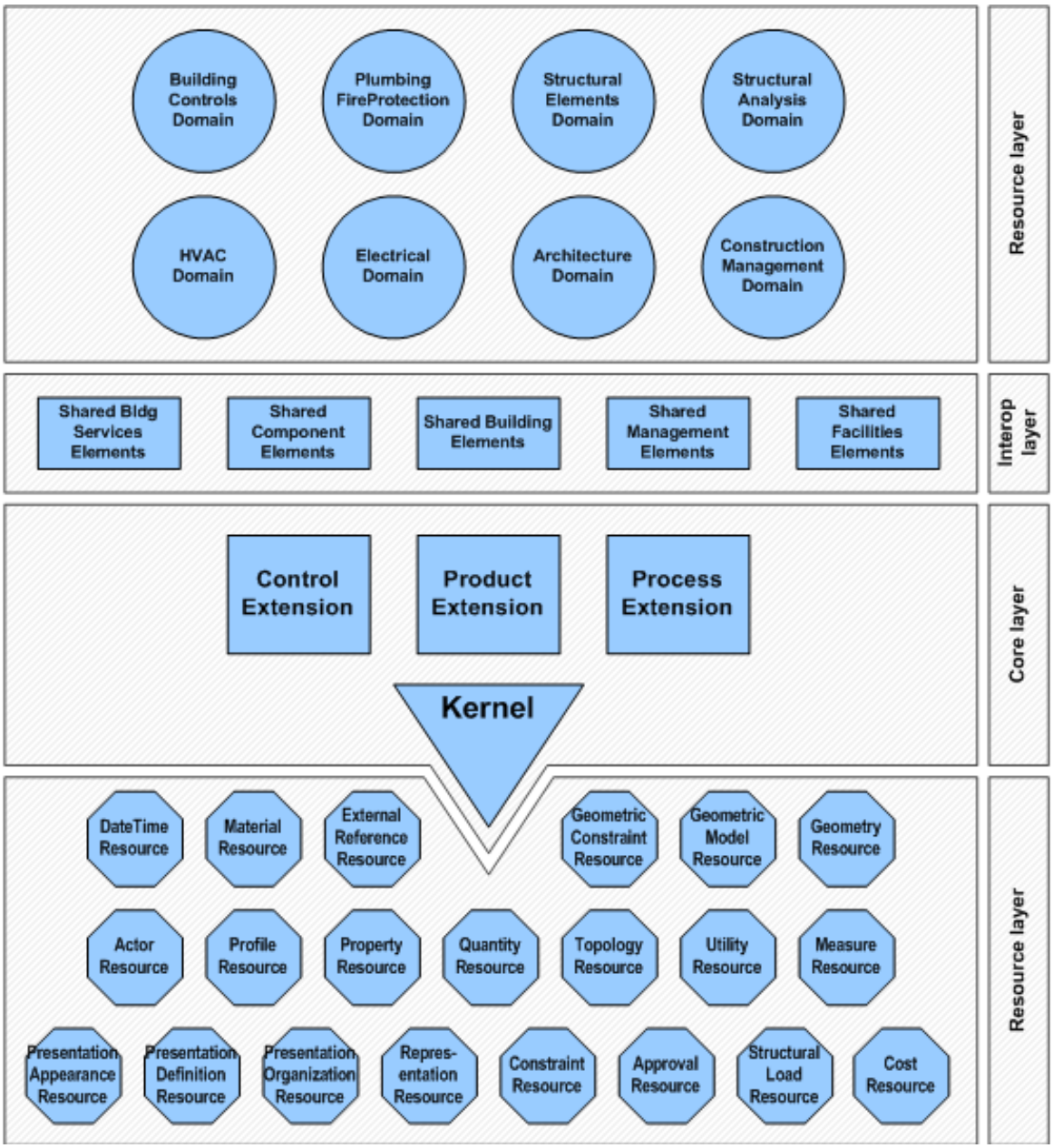

Figure 2.6: IFC data schema architecture [39].

- **Resource layer** — the lowest layer includes all individual schemas containing resource definitions

- **Core layer** — the next layer includes the kernel schema and the core extenstion schemas, containing the most general entity definitions, all entities defined at the core layer, or above carry a globally unique id and optionally owner and history

information

- **Interoperability layer** — the next layer includes schemas containing entity definitions that are specific to a general product, process or resource specialization used across several disciplines, those definitions are typicly utilized for inter-domain exchange and sharing of construction information;
- **Domain layer** — the highest layer includes schemas containing entity definitions that are specializations of products, processes or resources specific to a certain discipline, those definitions are typically utilized for intra-domain exchange and sharing of information.

Internal structure of devices is described using nested elements. For example, chiller shown in the figure 2.7 is composed from evaporator, compressor, condenser along with some valves and control system with actuators and sensors of temperatures and pressures. Those elements can be sources of information for virtual sensors or fault detection algorithm.

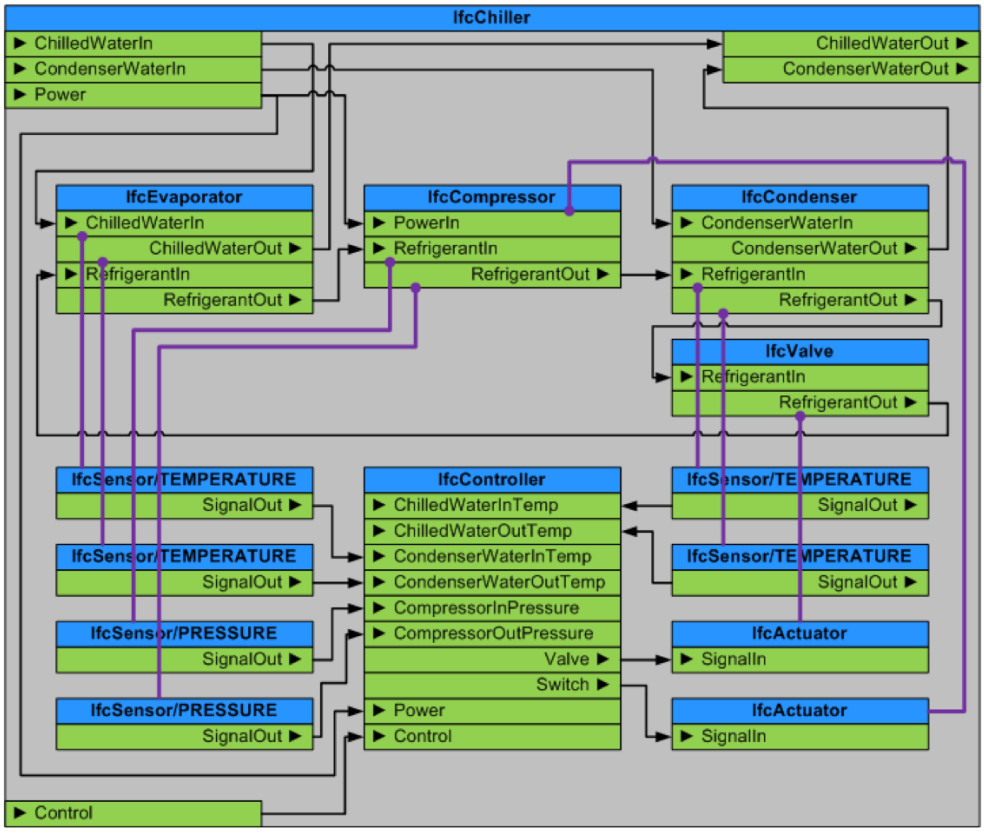

Figure 2.7: Chiller representation in IFC [39].

2.3 HVAC Systems in Buildings

HVAC systems used in commercial buildings come in a wide range of designs and sizes. Nevertheless, they are typically composed of the same basic parts [45].

- Hot water plants (comprising boilers and steam-to-water heat exchangers)
- Chilled water plants (comprising chillers and cooling towers)
- Air distribution plants (comprising air handlers and fan coils)
- Auxiliary devices (such as pumps and fans)

The basic principles of HVAC operation (i.e. the underlying physics, thermodynamics, etc.) are well described in ASHRAE Fundamentals [30]. Specific types of HVAC equipment and their individual components (valves, dampers, fans, etc.) are described in detail in the ASHRAE Handbook [46]. Extensive knowledge of heating and cooling of buildings was written by Kreider at al. [47].

Great variability of HVAC systems does not enable their easy categorization. I will attempt to sum up the main categories of HVAC systems, focusing primary on those HVAC devices, which are responsible for air conditioning (i.e. heating, cooling, humidification, and dehumidification) and distribution. This includes the following equipment types [30, 46]:

- **Air Handling Unit (AHU)** - AHU is responsible for intake of fresh outdoor air and its conditioning to yield the supply (i.e. temperature and humidity). AHUs are often used in large buildings with complex hierarchy (e.g. several floors and multiple sections). The AHU is typically located outside the conditioned area in a basement, penthouse, or service area. The AHU may be designed to supply a constant air volume or a variable air volume for low-, medium-, or high-velocity air distribution.

  Central system features: The conditioned air is fed either directly into the zone, it is typically used for low-velocity applications.

  Decentralized system features: The conditioned air is fed either into the downstream equipment.

  Single duct: contains the main heating and cooling coils in a series, a common air temperature feeds all downstream equipment.

  Dual duct: contains the main heating and cooling coils in parallel or series-parallel, a separate cold and warm air duct distribution system.

  One zone system: one output from AHU for all zone.

  Multizone system: more output from AHU for individual zone.

- **Roof Top Unit (RTU)** - RTUs are typically used in smaller buildings with simple a structure (e.g. retail stores, supermarkets, and restaurants). An RTU is also referred to as packaged HVAC equipment since it is standalone equipment capable of heating, cooling and air-conditioning. RTUs are basically AHU units for central system features.
- **Variable Air Volume (VAV) box** - VAVs are terminal devices in decentralized system features. Input for VAV is air from AHU unit, but VAV enables preparation of air for a particular zone. VAV terminal units are fitted with automatic controls heating coil, cooling coil and fan. VAVs are responding to changes of outdoor conditions.
- **Fan Coil Unit (FCU)** - the FCU is an in-room terminal unit system. FCU includes a central air-conditioning equipment, a duct and water distribution system, and a room terminal. Larger spaces may be handled by several terminals. Generally, the supply air (from AHU) volume is constant. These units must be properly controlled by thermostats and FCUs do not respond to changes of outdoor conditions.

AHU configurations that can be classified into different categories regarding major components types (e.g. using fans of either constant or variable speed) and based on the absence/presence of specific components (e.g. the heat wheel, the preheat coil, and the reheat coil).

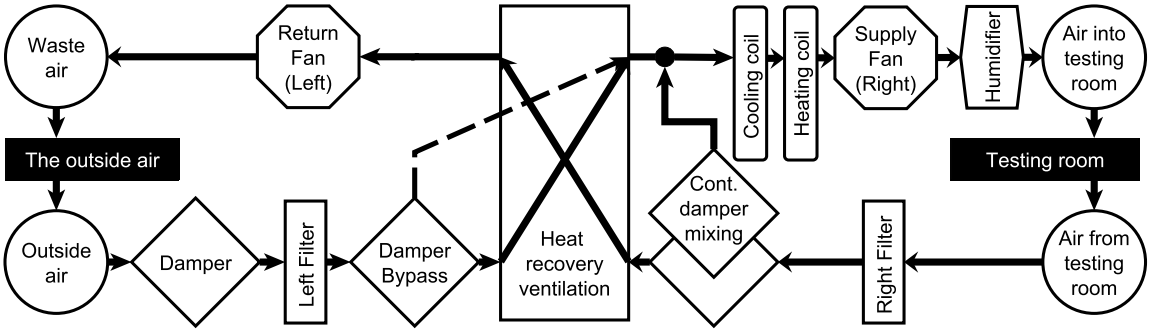

Figure 2.8: Example of AHU configuration.

Figure 2.8 depicts a simplified scheme of AHU. In the depicted unit, the air coming back from zones (driven by the return fan) is partially exhaust from the HVAC system (typically outside) and the rest is mixed with the incoming outdoor air. The mixture proportion is controlled by the damper mixing. The mixed air is driven by the supply fan through the cooling, heating coil and humidifier and is supplied to the zone. Described unit is experimental AHU of department of Microenvironmental and Building Services Engineering. I have this unit at disposal for experiment and it is enlarged on my publications [A.4, A.6].

2.4 Fault Detection and Diagnosis for HVAC

FDD is a branch in automatic control engineering, concerned with processes of identification faults of physical systems and diagnosing their causes. This part will be focused on FDD methods used in HVAC systems. A fundamental review article on FDD for building systems was written by Katipamula and Brambley [3, 8]. They call attention to the fact that although considerable growth in research into FDD for buildings has occurred, still only few commercial implementations are used. One presumed reason is lack of adequate sensors installed on buildings systems and lack of infrastructure to gather data from existing building automation systems. The doctoral thesis by Li describes FDD method for RTU unit [48]. Li used a lot of data from sensors, which are not commonly available in commercial HVAC systems. For this reason Li's methods are not all-purposed.

There are a number of extensive studies on HVAC system failures[49, 50, 3, 19, 48]. Brambley, Fernandez et al. are presenting in their work an extensive HVAC system bug report. This report is basic material for following description of typical HVAC errors. FDD methods can be categorized into three large groups, namely:

- **Data-driven (Process history based):**

  Black-box: diagnostic rules are derived statistically from large amount of measured data.

  Gray-box: use engineering knowledge to specify the mathematical description of systems, but parameters of the system are determined from process data.

- **Knowledge-based (Qualitative model-based):** Qualitative models are models consisting of qualitative relationships derived from knowledge of the underlying physics. This approach includes the rule-based system and models based on qualitative physics.

- **Model-based (Quantitative model-based):** Quantitative models are sets of quantitative mathematical relationships based on the underlying physics of the processes. These methods include those based on detailed physical models and models of the physical processes.

FDD is usually executed in the following three steps [13, 19, 51]:

- **Fault detection** - Determination of the faults present in a system (identification of an abnormal state of the system) and the time of detection.

- **Fault isolation** - Determination of the kind and location of a fault. Finding the root cause of a fault.

- **Fault identification** - Determination (or estimating) of the fault size and time-variant behavior of a fault.

From broad area of existing FDD methods, I will focus on category of qualitative model-based methods. Specifically on **AHU Performance Assessment Rules (APAR)**. It is a diagnostic tool that uses a set of expert rules derived from mass and energy balances exploiting the values of observed variables, control signals and occupancy information as an input to detect common faults in air-handling units. APAR rules are derived using qualitative models, similar to the approach used by Glass et al. [52]. The model-based approach by Glass et al. uses outdoor, return and supply air temperatures, control signals and physical rule to detect faults in multi-zones AHU with VAV units. Furthermore, APAR rules are similar to the rules used by Katipamula et al. [53]. APAR was introduced by House at al. (2001) in his work [3]. These principles were later validated and implemented as an FDD system by Schein at al. [54, 55, 56]. The authors introduced the APAR for detecting abnormal system behaviour. APAR rules were tested by Han and Chang for VAV unit [57].

The APAR rules are grouped into subsets based on the HVAC operating mode to which they apply. HVAC mode is identified by control signals and occupancy information. An example of fault detection rules:

$$T_{\mathrm{oa}} > T_{\mathrm{sa,s}} - \Delta T_{\mathrm{sf}} + \epsilon_{\mathrm{t}} \tag{2.1}$$

$$T_{\mathrm{sa}} > T_{\mathrm{ra}} - \Delta T_{\mathrm{rf}} + \epsilon_{\mathrm{t}} \tag{2.2}$$

$$T_{\mathrm{sa}} < T_{\mathrm{ma}} + \Delta T_{\mathrm{sf}} - \epsilon_{\mathrm{t}} \tag{2.3}$$

$$|u_{\mathrm{hc}} - 1| \leq \epsilon_{\mathrm{hc}} \text{ and } T_{\mathrm{sa,s}} - T_{\mathrm{sa}} \geq \epsilon_{\mathrm{t}} \tag{2.4}$$

where T_{oa} is the outdoor air temperature, T_{sa} the supply air temperature, $T_{\mathrm{sa,s}}$ the supply air temperature set point, T_{ra} the return air temperature, T_{ma} the mixed air temperature, ΔT_{sf} the temperature rise across the supply fan, ΔT_{rf} the temperature rise across the return fan, ϵ_{t} the threshold for errors in temperature measurements, ϵ_{hc} the threshold parameter for the heating coil valve control signal, u_{hc} the normalized heating coil valve control signal $[0, 1]$ (where $u_{\mathrm{hc}} = 0$ indicates the valve is closed and $u_{\mathrm{hc}} = 1$ indicates it is 100% open).

An example of fault detection rules for the mode of cooling with outdoor air within an HVAC system are described by equations 2.1 and 2.2. Rules for the mode of heating are described by equations 2.3 and 2.4. If one of rules is true, it implies the existence of a fault. The fault detection logic should handle transient states (since the system response to control change-over may take some time due to the slow dynamics of the heat exchange process) and should not produce false alarms within these periods. Several root causes can cause violation of a single rule. Hence, a combination of fault isolation and identification

(i.e. fault diagnostics) must be exploited in order to discover the underlying root cause. Diagnostics of a single fault is usually based on multiple symptoms (e.g. observed variables, control signals, and occupancy status).

Authors ascertained that some faults could not be detected under certain operating conditions because the control system was able to mask the problem or because sensor data needed to detect the fault is not commonly available in commercial systems. Conversely, the presence of additional sensors would expand the rule set and provide an opportunity to either detect more faults, or to detect faults during modes of operation in which they would normally be hidden. The APAR rules can be combined with next FDD methods to achieve better results.

2.4.1 HVAC Fault Categorization

HVAC faults can be divided into several categories [13]:

- **Design faults** i.e. for example a wrong installation of a device (this will not be dealt with further).
- **Hardware faults** can be further categorized:

  Abrupt faults i.e. stuck damper or a stuck valve on supply water.

  Gradual faults i.e. equipment is mechanically damaged due to wear, contamination by dirt and rusting. This category include **performance degradations** i.e. equipment still operates, but with reduced efficiency due to wear and contamination by dirt.
- **Control inefficiencies** (e.g. inefficient control due to incorrectly chosen control strategies and inappropriate scheduling)
- **Sensor faults** (i.e. invalid values coming from the sensor due to sensor failure, drift, bias, etc.)

Table 2.1 provides concrete examples of HVAC faults [51, 56]. HVAC faults that do not cause a loss of comfort or excessive energy consumption may remain undetected for a long time period. The following AHU/RTU faults will be of primary interest for my thesis.

Hardware Faults:

Fault Type	**Fault Name**	**Note / Example**
Hardware Fault (Equipment Faiture)	Cooling failure	Cooling valve is leaking or stuck (open, closed, etc.)
	Heating failure	Heating valve is leaking or stuck (open, closed, etc.)
	Economizer failure	Stuck / leaking / by-passed outdoor air damper
	Fan malfunction	E.g. fan motor failure
	Refrigerant issue	Refrigent overcharge / undercharge / leak
	Liquid slugging	Liquid floodback, liquid line restriction
	Motor fault	For refrig. compressor, pump, etc. bearing fault, slipping belt, etc.
Control Inefficiency	Control fault cooling	Too hot or too cold due to controller (e.g. schedule override)
	Control fault heating	Too hot or too cold due to controller (e.g. schedule override)
	Post occupancy operation	Equipment running overnight, on weekends, etc.
	Scheduling fault	Early / late start or shutdown
	Inefficient damper control	Cooling used even though natural ventilation would save energy
	Simultaneous heating and cooling	This does not apply dehumification
	Wrong control mode	Condensing boiler in not-condensing mode
	Short cycling	Frequent cycling (on-off, off-low-high) Short uptime / downtime
	Poor PID tuning	Oscillatory control signal, overshoots, sluggish response
	Permanent set point offset	Missed set point e.g. due to undersized equipment
	Wrong set point	Issue in set point reset strategy (disabled, wrong parameters)
	Lack of synchronization	Boilers are running, but pumps are OFF (or vice versa)
	Lack of cooperation	Heating and cooling; multiple boilers lead-lag fault
Performance Degradation (Reduced Efficiency)	Air filter clogging	
	Water pipe scaling	
	Fouling	Condenser / evaporator fouling
	Reduced boiler efficiency	Combustion efficiency; various types of losses
	Reduced HEX effectiveness	
	Reduced fan efficiency	
	Reduced pump efficiency	
	Reduced COP	COP = Coefficient of Performance

Table 2.1: List of HVAC faults containing fault categories and examples [49, 50].

- Cooling and heating failure: A possible root cause of this failure is that the heating and cooling coils can leak or a valve is stuck in the open or closed position or somewhere in between.

- Economizer failure: Economizer cycle is an operating practice utilizing free cooling by the outdoor air if applicable. If the outdoor air is cool enough, mechanical cooling can be shut down and the temperature setpoint value is reached by simple mixing the outdoor air with the return air. The economizer failure fault means that the outdoor air damper is leaking, stuck or being blocked by the maintenance staff in order to try to resolve a complaint. A permanently open damper causes energy waste due to unavailability of free precooling or excessive ventilation when it is hot outside, and also can result in frozen unit coils or even damage of the occupied spaces during the heating period.

- Fan malfunction: Fans provides the work needed for driving the air through the system (i.e. the filtration system, the heating and cooling coils, ductwork, and the conditioned space) in order to meet the heating/cooling requirements. The fan malfunction error means that the supply fan fails to provide sufficient airflow into the zone due to a mechanical failure or reduced efficiency. As a consequence, the zone temperature decreases during the heating season (or increases in the air-conditioning season). The controller reacts to this by commanding the heating (or the cooling) to increase (or decrease) the temperature. This results in excessively high (or low) supply air temperature.

Control Inefficiencies:

- Cooling/heating control fault: This fault is typically caused by a manual override of the control strategy. In such a fault the control strategy does not propagate the signal to the data warehouse where it can be used by the FDD module. As a consequence, the zone temperature appears too hot or too cold with respect to the warehouse setpoint value. e.g. temperature of inlet air into VAV units is high, but low temperature of VAVs output is required.

- Inefficient damper control: This fault means that the mechanical cooling is used even though it could be shut down during the economizer cycle.

- Simultaneous heating and cooling: This fault signifies simultaneous heating and cooling due to a poor control strategy.

Performance Degradation:

- Air filter clogging (or plugging) - By removing dust and dirt from the air stream, filters protect HVAC equipment from fouling (accumulation of dirt from air flow on the surface of heating/cooling coils leads to reduced heat transfer). A clogged filter restricts air flow and thus causes a higher pressure drop within the system. In constant-volume air handling systems, filter slogging implies decrease in air quality. In variable volume systems, this causes higher energy consumption of the fan, which has to work more to drive the air through the system and thus meet the heating/cooling requirements.

2.4.2 Typically Missing Sensors

A major challenge for FDD methods (and for virtual sensors) is replacing information that is needed for fault diagnostics. This problem may be temporary (e.g. due to data acquisition failure) or permanent (e.g. data is not available because the HVAC system is not equipped with certain sensors). The goal of this section is to provide examples of typically available and missing sensors and in this way provide use cases for virtual sensors.

Table 2.2 provides an overview of typically available and missing information in HVAC systems (i.e. sensor measurements, control setpoints, control signals, etc.). The information are classified into three categories:

- Common (i.e. information that are almost always available; Figure 2.9 shows placement of original sensors in our experimental unit.)
- Optional (i.e. information that may or may not be available depending on the system configuration)
- Missing (i.e. information that are seldom/never available.)

The missing and optional sensors, which are listed in Table 2.2, can allow to use of a wide range of FDD and efficiency monitoring analysis, which are not yet used in practice. Replacement of missing sensors by virtual sensors would enable to extend APAR rules [54, 55, 56]. Hence, these points represent use case scenarios of for virtual sensors computation. New rules of APAR can be developed afterwards.

- **Return air temperature** - This point allows for more reliable and more accurate estimation of the mixed air temperature.

Data Point Category	**Data Point Name**	**Related Equipment**
Global	Building occupancy status	All
	Zone occupancy status	All
	Real-Time tariff (Electricity price)	All
Electricity Consumption	RTU / AHU consumption	RTU, AHU
	Supply / return fan consumption	RTU, AHU
Temperatures	Return air temperature	RTU, AHU
	Mixed air temperature	RTU, AHU
	Temperature between coils	AHU, RTU, FCU, VAV
	Boiler room temperature	Boiler, Hot water plant
	Flue (gas) temperature	Boiler
Flows	Supply air flow	AHU, RTU, FCU, VAV
	Supply water flow	Boiler, Hot water plant
	Fuel (gas) flow	Boiler
Zone Conditions	Zone air humidity level	All
	Zone air CO2 level	All
Control Signals	Supply fan speed control signal	AHU, RTU, FCU, VAV
	Pump speed control signal	Hot / chilled water plant
	Pump runtime status	Pump, hot water plant
	Firing rate	Boiler
Setpoints	Zone air temperature	AHU, RTU, FCU, VAV
	Supply air temperature	AHU, RTU, FCU, VAV
	Supply water temperature	Boiler
Refrigeration	Compressor current	RTU
	Compressor status	RTU

Table 2.2: Summary of typically missing sensors on HVAC system [49, 50].

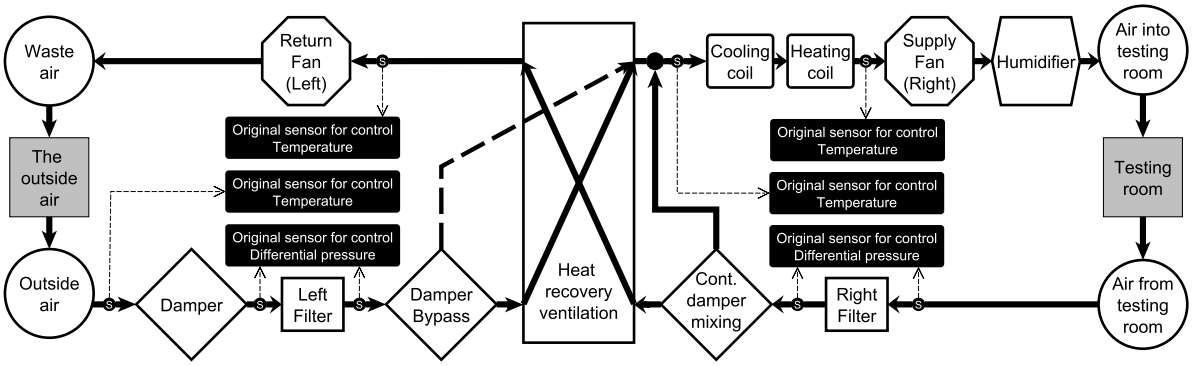

Figure 2.9: Typically available sensors in an RTU

- **Mixed Air Temperature** - This point is essential for diagnostics of the outdoor air damper position problem due to either hardware fault (i.e. stuck damper) or control fault (i.e. inefficient ventilation).
- **Temperature Between Coils** - This point is needed for diagnostics of faults related to cooling and heating valves (or stages). It can be used for distinguishing among the following faults: cooling/heating valve stuck open, cooling/heating valve stuck closed, leakage of cooling/heating valve. This point is also useful when additional coils (e.g. preheat coil, reheat coil) are present in the system.
- **Supply Air Flow** (or Supply Air Differential Pressure) - This point is essential for quantifying the energy balance equation (i.e. for having complete understanding of the energy supplied versus energy delivered). It can be used for monitoring of many faults (e.g. unnecessary mechanical cooling due to inefficient ventilation, excessive air flow, and low air flow).
- **Supply Fan Speed Control Signal** - This point is essential for estimation of the supply air flow.
- **Zone Air Temperature Setpoint** - This point is necessary for detection of all faults related to zone comfort (e.g. too hot or too cold in the zone) due to either control fault (namely a controller error or control override) or hardware fault (namely a stuck/leaking valve or fan malfunction).

2.5 Use of Virtual Sensors and BIM in FDD

The main contribution of this dissertation is the connection between BIM and FDD. **The relationship between BIM and FDD** can be **virtual sensors**, witch inputs parameters are described by **ontology**. Ontology is a unifying element between VS inputs a BIM. Virtual sensors can be created and calibrated automatically based on information from BIM, and these virtual sensors can be used for FDD.

Ploennigs et al. made virtual sensors for estimation of a room's heat consumption [59]. Ploennigs highlights using BIM for reducing the effort for simulations. Zimmermann et al. used BIM (IFC format was used) for creating heat flow model (HFM) [58]. At first IFC description of the building is transformed into a graphical representation and IFC missing components (as sensor and description of these components) are added by the user. From expanded graphical representation model in XML format is created. At second run-time FDD system from an XML-based HFM model is created. The generator is implemented in Java.

The HFM model is a graph with nodes that correspond to HVAC system components (coils, fans) and arcs that correspond to mass flow connections (ducts or electrical energy flows in power lines). The approach is based on modeling the flow processes of an HVAC system and comparing simulated data dynamically with measured temperature, humidity, and pressure data in addition to flow data. Faults in the system will show up as simulation measurement value differences that exceed given thresholds. Method was tested only on simulated data. These faults were included in data for testing: Offset of temperature sensors, stuck of dampers and stuck of valves. Many of faults were detected.

BIM contains all entities of the HVAC system [39], building construction, electrical wiring diagram et cetera. BIM is supported by extensive design studies as ArchiCAD and Autodesk Revit software. Due to this fact, a lot of visualization tool exists. The example of a large system visualization is shown in figure 2.10. Thanks to visualization, verifying the quality of BIM processing is easy. View information about individual HVAC system elements is enabled by visualization tools. Verification of usability information for virtual sensors and FDD is possible, without having to know BIM syntax.

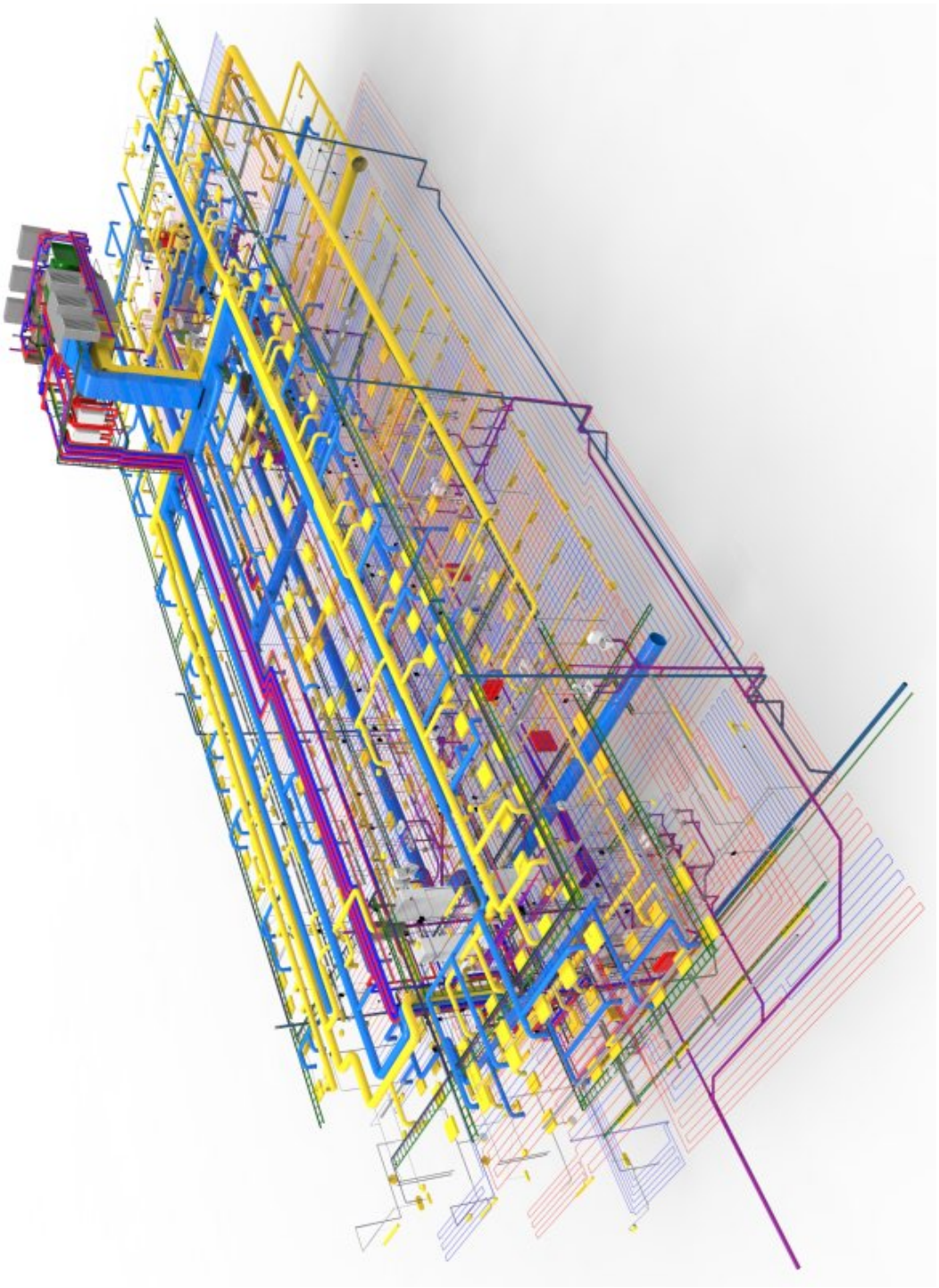

Figure 2.10: Example of HVAC system visualization fro BIM. (Source: remars.co.uk)

Chapter 3

Aims of the doctoral thesis

The purpose of this thesis is to propose a particular solution for energy saving in commercial buildings with HVAC (Heating, Ventilation, and Air Conditioning) system thanks to FDD (Fault Detection and Diagnostics) methods and performance monitoring.

Based on the research of state of the art, two main challenges were identified: the absence of the sensors needed to diagnose the HVAC and the problematic configuration of the FDD methods for specific building (for example, building geometry, equipment parameters, etc.).

VS (Virtual Sensors) represent a promising alternative to missing real sensors needed for FDD; on the other hand, their configuration for a specific application is complex and costly. For the automated configuration and parameter setting of FDD methods and Virtual Sensors, information about the building geometry, materials, topology and equipment are needed and can be extracted from building information model (BIM). The aim of the thesis is to develop a framework for the automated design of virtual sensors for monitoring, fault, and degradation detection.

The objectives of the thesis are as follows:

- The main objective is to propose a **novel approach for automatic design and configuration of virtual sensors** using the building information model (BIM). The main objective is separated into two objectives (two types of virtual sensors using different BIM information):
  - To develop a virtual sensor with automated configuration using information about the geometry and material properties provided by BIM
  - To develop a virtual sensor with an automated parameter setting using information about the HVAC equipment extracted from BIM
- To validate the proposed virtual sensors experimentally.

Chapter 4

Automatically configured virtual sensor using information about the geometry and material properties provided by BIM

The methodology described in this chapter enables the automatic exploitation of the information provided by BIM (Building Information Model) for FDD (Fault Detection and Diagnostics) [A.5]. In the framework developed within this thesis, geometric information about the building from IFC BIM is retrieved and saved into the data structure. Geometric information about windows, doors, ceilings and walls is included. Data structure serves as an input for a **virtual sensor of the temperature in zone**. The temperature of the zone is estimated on the basis of information from IFC BIM and temperatures in surroundings of the zone.

4.1 Building geometry extraction from IFC BIM

A large number of entities is contained in IFC. Some of them represent objects in reality and some are used to describe these objects' attributes. IFC entities enable the description of all objects and properties of those objects from which the building is constructed.

In Fig.4.1 is shown an example of IFC hierarchy of the standard wall. It starts in a black rectangle where the list of all objects (entities) belonging to one storey is shown. This list is contained in *IfcRelContainedInSpatialStructure* entity. In the following diagram the IFC hierarchy of one wall is shown. This hierarchy is represented using *IfcWallStandardCase*.

The shape and placement of wall is determined using *IfcLocalPlacement* and *IfcProductDefinitionShape* entity. The exact coordinates of wall points are accessible by browsing

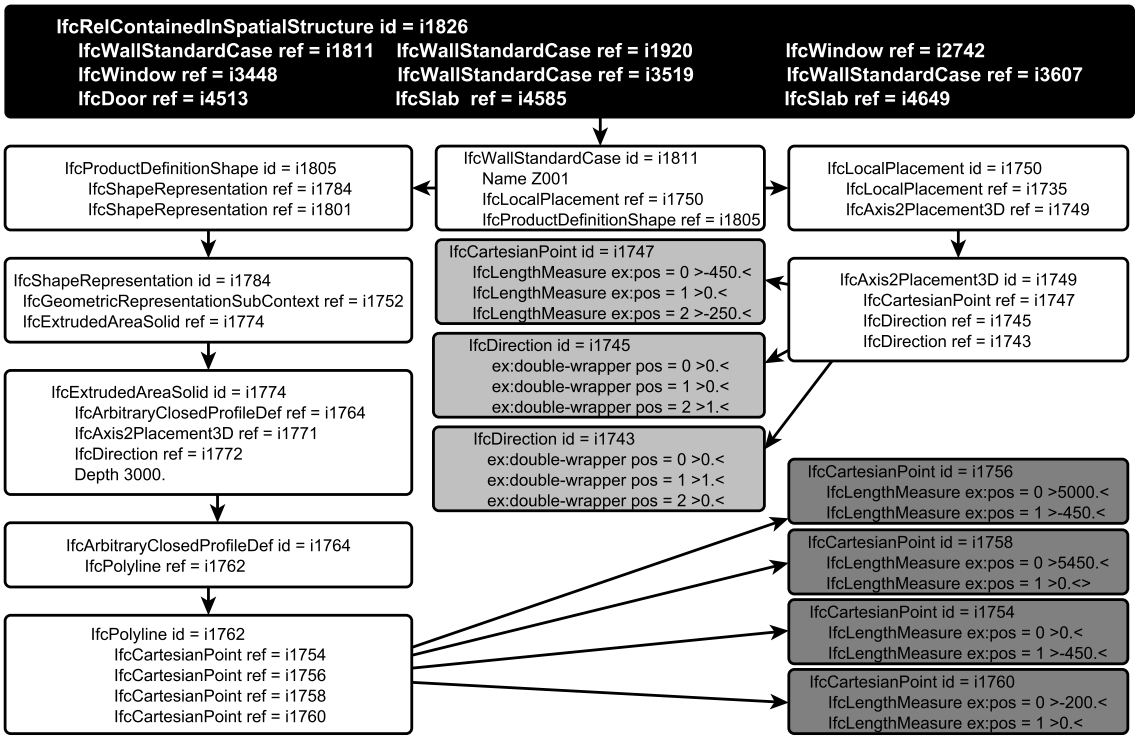

Figure 4.1: An example of IFC hierarchy for IfcWallStandartCase

the tree hierarchy from *IfcLocalPlacement* or *IfcProductDefinitionShape* to *IfcCartesianPoint* and *IfcDirection* through the other IFC entities. Each point of the wall is determined by three parameters: the relative coordinates giving the dimensions of the wall, the relative coordinates providing the location of the wall and direction vectors which describe the orientation of this local system. The required output is composed of these three parameters of all points.

Other processed elements of the buildings are the doors and windows. These objects are described using *IfcWindow* and *IfcDoor* entity. The dimensions of these object are directly accessible through attributes OverallHeight and OverallWidth. Other important information is accessible through *IfcOpeningElements* where every opening element is assigned to one wall.

4.2 Retrieval of information from IFC

In the next chapter whole process from architect's hands to tables with calculated points coordinates of all walls is described. The whole procedure is shown in Fig.4.2. The first

step is the creation of an architectural drawing by Autodesk Revit. The second step is the export of the architectural drawing as an ifc file.

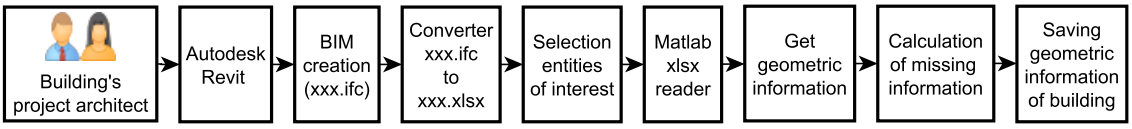

Figure 4.2: The diagram of whole process of obtaining data from IFC file

After the *.ifc file is created by Autodesk Revit, it is a text file with thousands of lines which are difficult to read. Therefore for unification and better readability is the *.ifc file preprocessed by IFC file analyzer. The IFC file analyzer is free software which generates spreadsheet in *.xlsx format. The spreadsheet is created with as many worksheets as the number of entities used in the *.ifc file and each row in one worksheet belongs one instance of this entity with its attributes.

When the spreadsheet with IFC data is created, the file is loaded to programmed Matlab reader and the data from entities of interest are extracted. As an output of programmed Matlab reader several tables are created with geometric information: a table with information about position of all points of walls, a table with information about position of all points of floors and ceilings, a table with assignment windows to walls and windows area and a table with assignment doors to walls and doors area. It is important to mention that the coordinates of all points of walls, floors and ceilings are relative to other point coordinates. So these points have not global coordinates. Therefore these loaded raw data is needed to be recalculated to global coordinates. After this, every point is simply determined by three coordinates. These known global coordinates of all walls points are further used to compute several information about building such as areas and volumes of walls or volumes of air in the rooms.

4.3 Virtual sensor of zone temperature

4.3.1 Heat models for estimating of the zone temperature

The basic core of virtual sensor is a grey box model, which was published by Andersen et al. [31]. The model was formulated as a system of stochastic differential equations and statistical methods which were applied for identifying, estimating and validating the model. The model is based on two equations:

$$C_{\mathrm{i}}\frac{\mathrm{d}T_{\mathrm{i}}}{\mathrm{d}t} = \sum \phi_{\mathrm{in}} - \sum \phi_{\mathrm{out}} \tag{4.1}$$

where C_{i} (J/°C) denotes the zone heat capacity, T_{i} (°C) is the zone temperature, ϕ (W) is the heat transfer and

$$C\frac{\mathrm{d}T}{\mathrm{d}t} = \sum_{x=1}^{n} B_{\mathrm{w}_x}(T_{\mathrm{j}_x} - T_{\mathrm{i}_x}) + \phi_{\mathrm{s}} \tag{4.2}$$

where C (J/°C) denotes the heat capacity, T (°C) is temperature, B_{w} (J/(°C · h)) is the thermal conductivity for a specific wall or floor w, T_{i} (°C) and T_{j} (°C) are the temperatures at each side of the wall or floor. ϕ_{s} (W) is the power from solar radiation and n (−) is the number of the wall and floor w.

Equation 4.1 describes temperature in the zone, which can be estimated as the sum of all heat transfers into and out of the zone. Equation 4.2 describes the total conductive heat transfer through the walls, floor and from solar radiation into the zone.

$$C = c \cdot V \cdot \rho \ ; \ B_{\mathrm{w}} = U \cdot S \ ; \ \phi_{\mathrm{s}} = I \cdot A \cdot k \tag{4.3}$$

where c (J/(kg · K)) is the specific heat capacity, V (m^3) is the object volume, ρ (kg/m^3) is the density of object, U (W/(m^2 · K)) is the coefficient of an external heat conductivity of an object, S (m^2) is the area of an object, I (W/m^2) is the solar intensity, A (m^2) is the area of a window and k (−) is the coefficient of permeability of windows ($k = 0,6$ was selected [31]).

$$I = I_{\mathrm{G}} \cdot \cos\gamma \ ; \ \cos\gamma = \sin h \cdot \cos\alpha + \cos h \cdot \sin\alpha \cdot \cos(a - a_{\mathrm{s}}) \tag{4.4}$$

where I_{G} (W/m^2) is the global solar intensity, h (°) is the elevation angle (measured from the horizon), α (°) is the aperture tilt angle of the window, a (°) is the azimuth angle (measured clockwise from the North) and a_{s} (°) is the azimuth angle of the window (measured clockwise from the North). The parameters of I (W/m^2) are shown in Fig.4.3. Equations 4.3 and 4.4 describe all necessary calculations for equation 4.2.

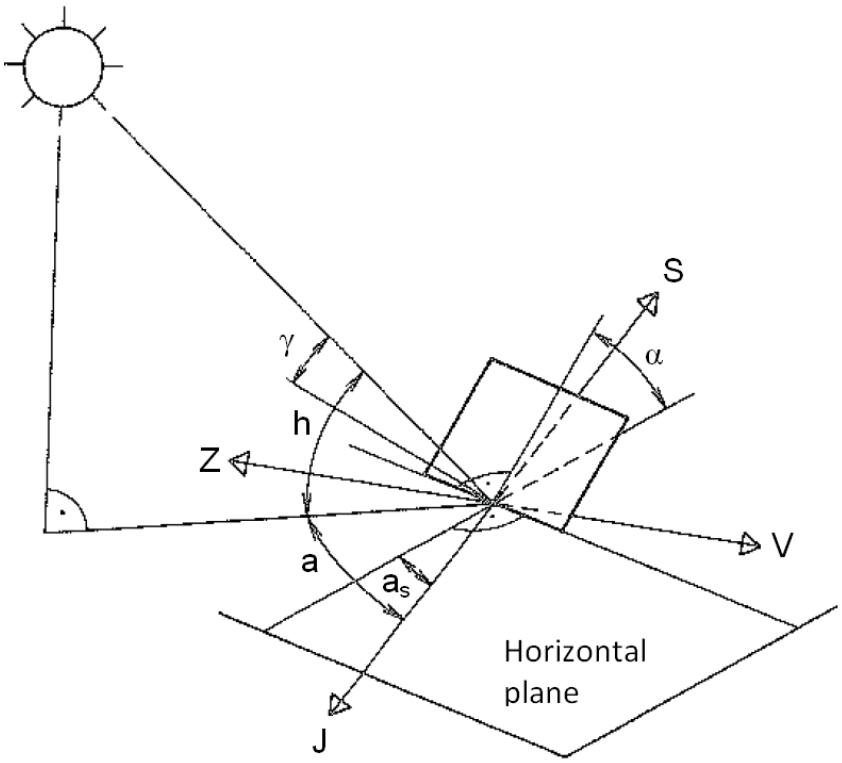

Figure 4.3: Calculation of the intensity of solar radiation

4.3.2 Test results

The virtual sensor was tested in real building. In Fig.4.4 a tested building in cadastral map is shown. This map was used for the verification of parameters a_s and α extracted from BIM. A detailed drawing of a tested building is shown in Fig.4.5 There is an original building drawing by the architect. A tested room (bedroom) is situated in the upper left corner in Fig.4.5.

In Fig.4.6 and Fig.4.7 graphic output (3D and 2D visualization of the tested building) of our software is shown. In these pictures the tested room is marked as r.1 (room 1) and is located in the lower left corner. The tested room was used as a storage area without internal heat source during the test. The tested building is fitted with a temperature sensor in each room and an outdoor temperature sensor.

The majority of parameters can be extracted from BIM. Namely: V, S, A, a_s and α. The next group of parameters are extracted by a link between building materials and specifications of materials. Namely: c, ρ and U. The type of material is extracted from BIM, but the specifications of the material are assigned by an established table.

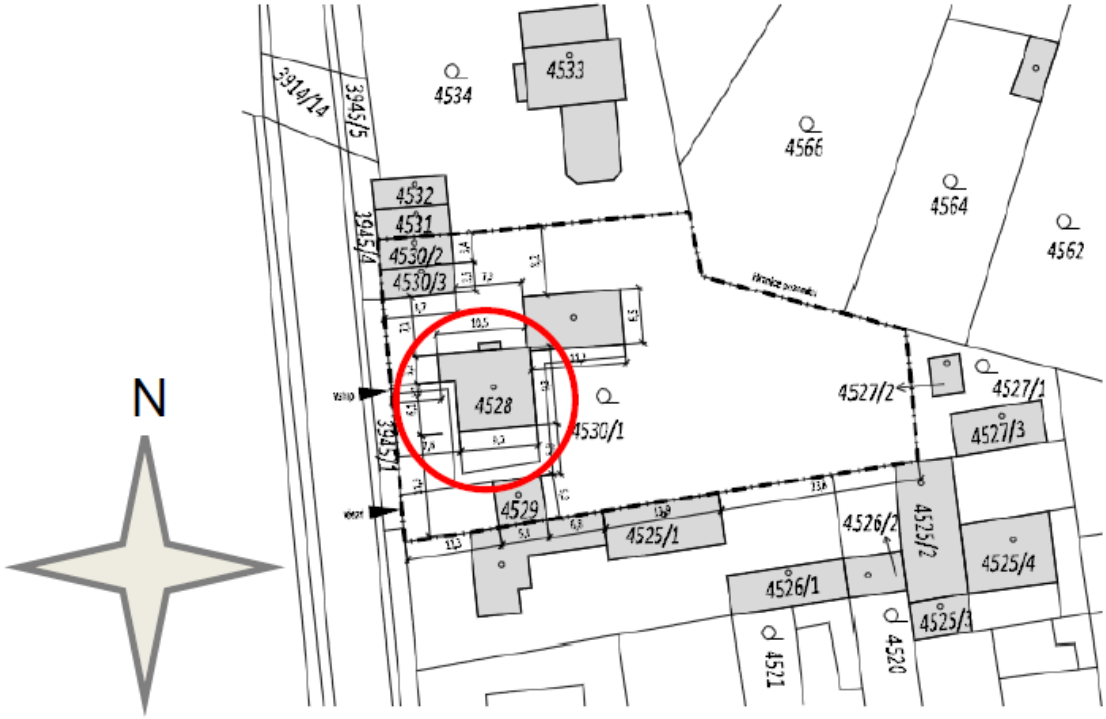

Figure 4.4: Tested building in cadastral map

The last group of parameters are actual real data. Ambient temperatures T_{i} and global solar intensity I_{G} have to be measured by real sensors. The global solar intensity can be extracted from nearby meteorological stations. The parameters of the sun's movement (in tested building area) are a prerequisite for the specification of h and a.

4.4 Conclusions

In Fig. 4.8. output of our model of the room is shown. The output of the model is compared with the real measured temperature in the tested room. The total test time was 31 days. The result of the test is optimistic; only the one significant difference shown as a peak measured in real temperature was caused by opening the door to the test room. The maximum difference between the calculated and the actual temperature is approximately $2°C$. The virtual sensor of zone temperature with automatic information extraction from BIM can be used, for example, to detect drift of a real sensor or to detect an open window or door in a room.

By measuring the real sunlight in around test building, a more accurate estimate of the temperature inside the test room could be obtained. For practical use of this virtual

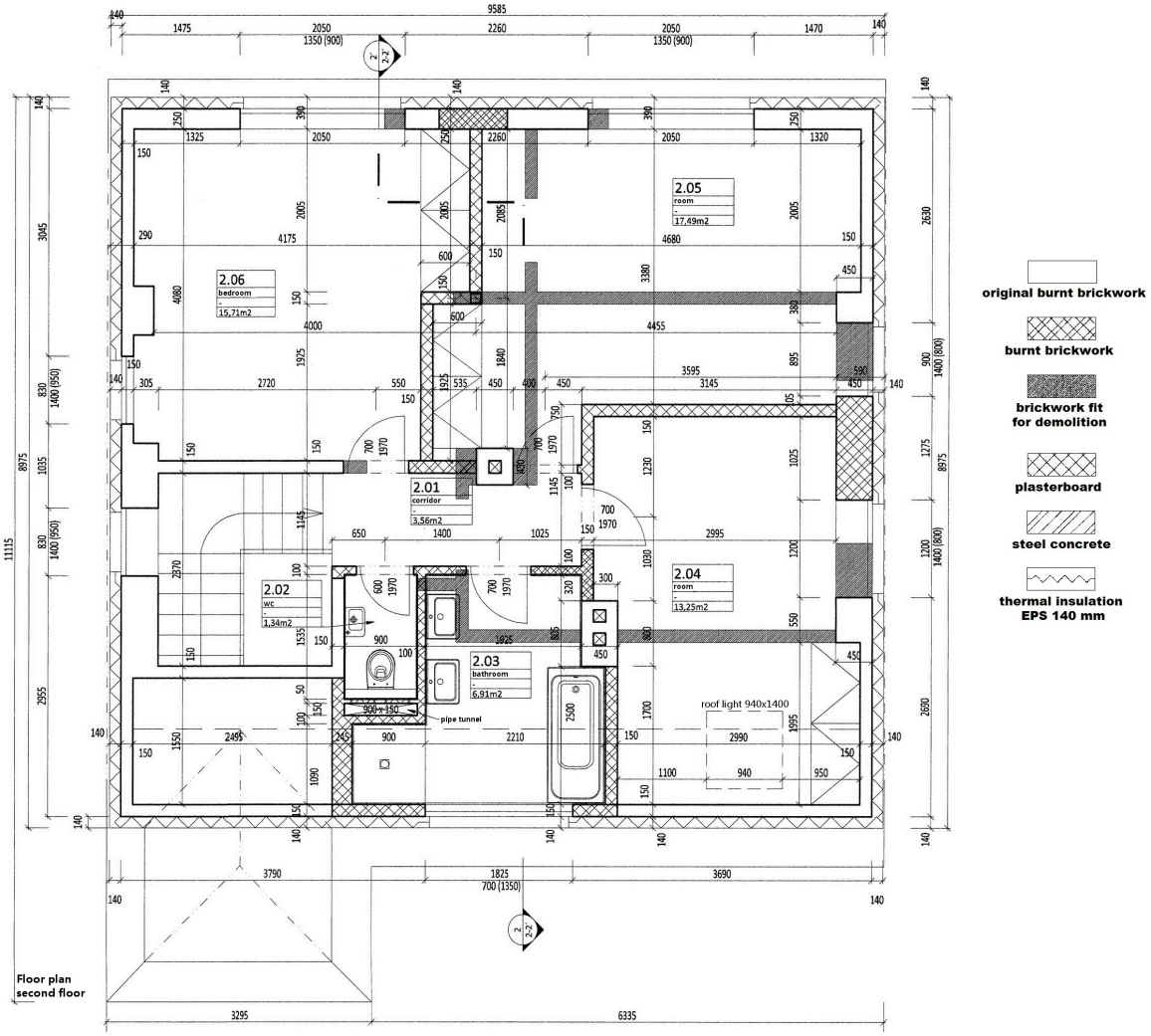

Figure 4.5: Architectural drawing of tested building

sensor, the VS (Virtual Sensors) must be extended by estimating the heat gain from the heating (or other sources of heat or cold).

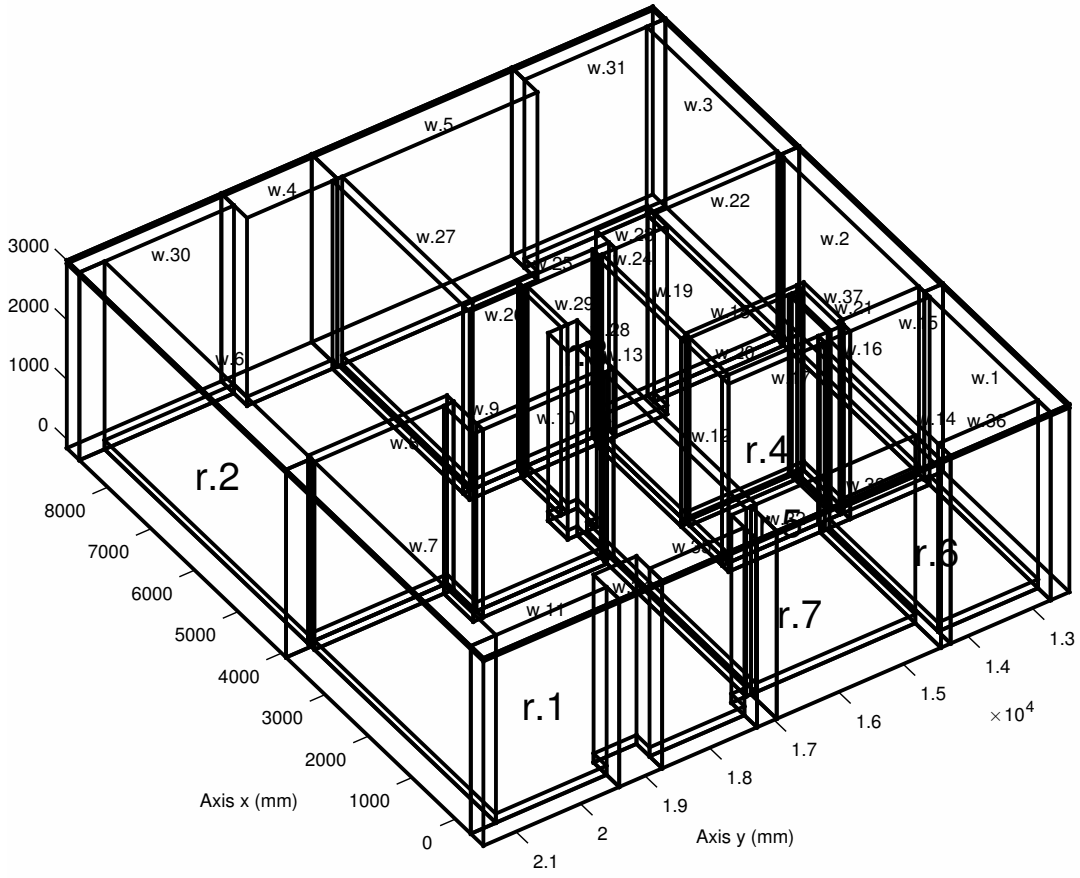

Figure 4.6: 3D visualization of tested building in Matlab

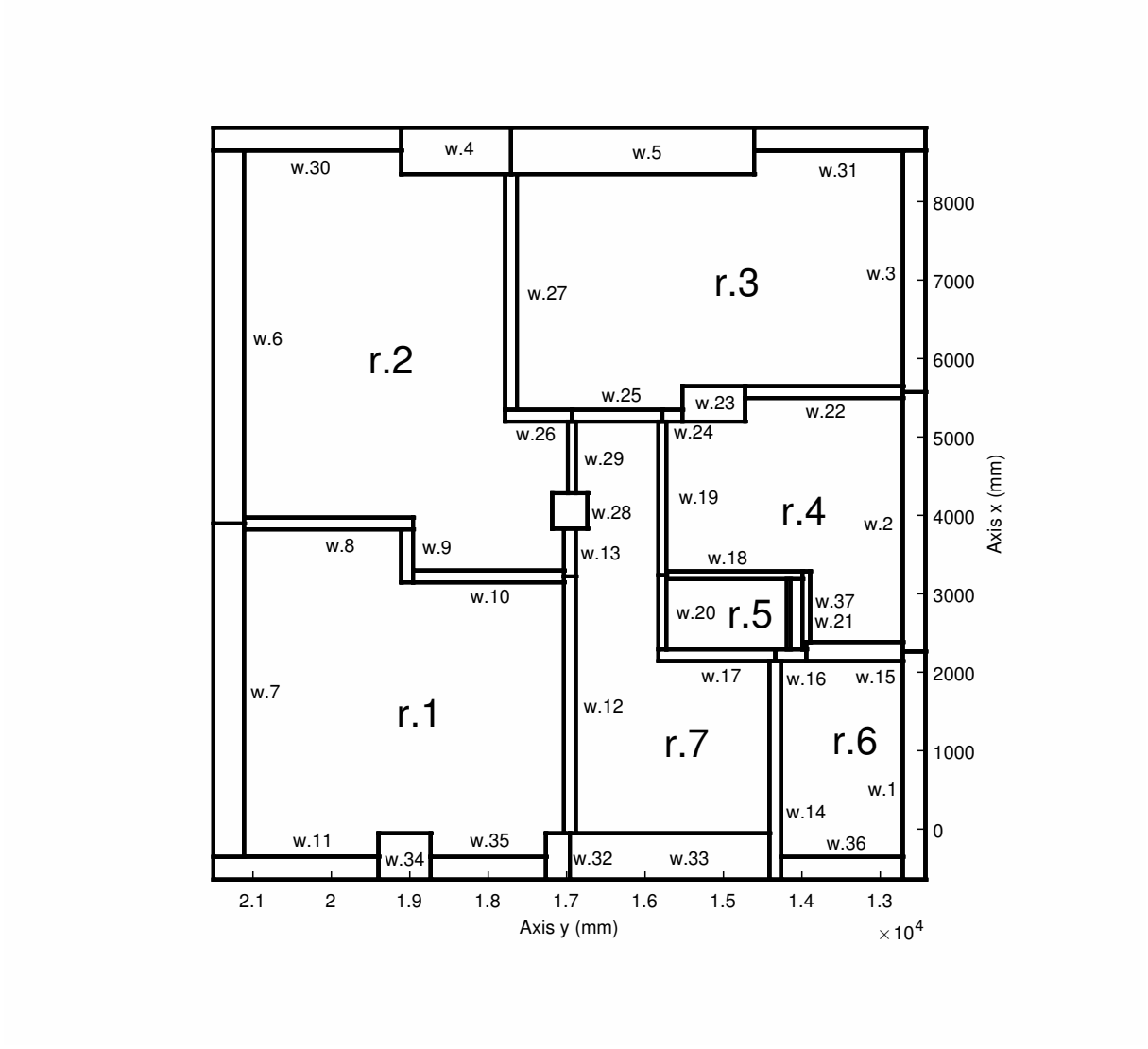

Figure 4.7: 2D visualization of tested building in Matlab

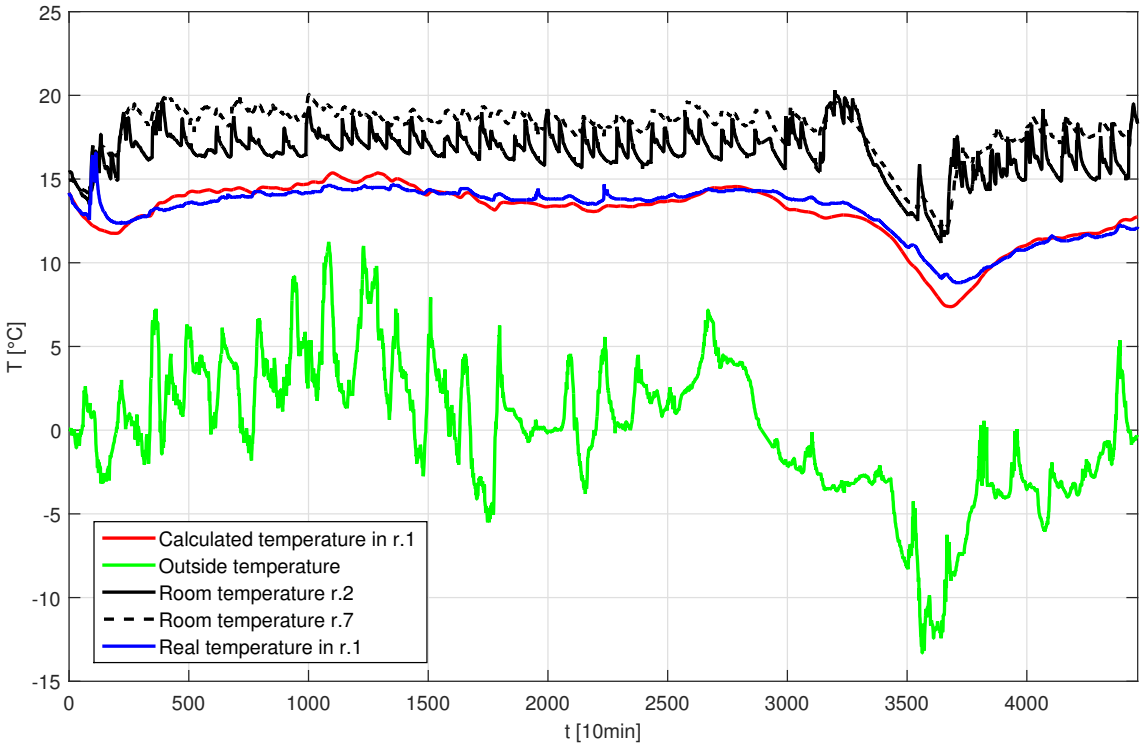

Figure 4.8: Output of model

Chapter 5

Automatically configured virtual sensor using information about the HVAC equipment provided by BIM

The methodology described in this chapter enables the automatic extraction of the information about the HVAC equipment provided by BIM (Building Information Model) for automatically configured virtual sensors. **Two virtual mass flow rate sensors** are presented. The **first-principle based VS** (Virtual Sensors) uses a simplified model of the recuperator, the **grey-box based VS** uses a performance curve of the recuperator.

5.1 Virtual mass flow rate sensor design

The models of virtual mass flow rate sensors described in this chapter are based on the heat balance of the recuperator. The recuperator is an air-to-air fixed-plate heat exchanger that utilizes the heat exchange between the inbound and outbound air flow. Recuperators save energy by reducing the heating (and cooling) requirements [30].

A recuperator usually consists of series of parallel plates made of aluminum, plastic, stainless steel, or synthetic fiber. Each pair of plates is connected on two sides to create a pass-through duct. These ducts are attached to each other and alternately rotated by ninety degrees. A different duct orientation separates the supply and exhaust air streams.

The heat flux between two fluids inside a recuperator can be estimated on the basis of measurements of temperature and other parameters, such as exchanger type, exchanger geometry, and the parameters of the fluid and mass flow rate. The converse is also true - the air mass flow rate can be estimated from temperature measurements and from knowledge of the parameters of the recuperator.

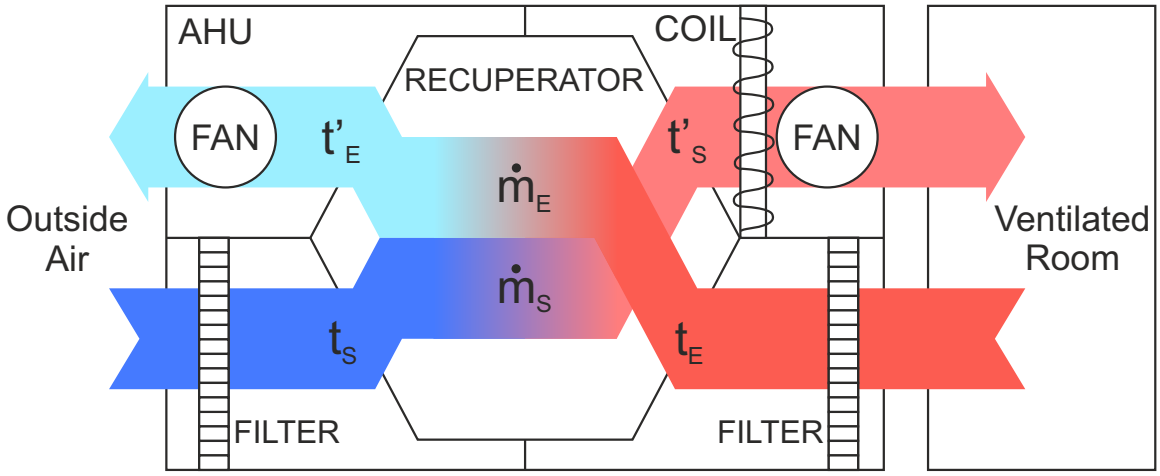

Figure 5.1: Generic scheme of Air Handling Unit with a recuperator.

Generic scheme of AHU (Air Handling Unit) with a recuperator (winter mode) is shown in the picture 5.1, where $\dot{m}_s$ is the mass flow of the supply air $\dot{m}_e$ is the mass flow of the exhaust air, t_s is the temperature of the supply air at the inlet of the recuperator, t'_s is the temperature of the supply air at the outlet of the recuperator, t_e is the temperature of the exhaust air at the inlet of the recuperator, and t'_e is the temperature of the exhaust air at the outlet of the recuperator

Main advantages of the proposed VS:

- It is based on simple physical principles, so no complicated model training is required.
- Our VS uses only temperature sensors, which are widely used in modern AHUs.
- Most recuperators have a similar structure, which simplifies sensor implementation.
- The recuperator itself has no mechanical parts, and is protected from both sides by filters. Its parameters used in VS are virtually constant during their lifetime.
- The proposed VS can be used in both winter and summer periods.

Recuperator parameters can be expressed as performance curves or as physical parameters (e.g. recuperator type, geometry or material used), two approaches to mass flow rate calculation are therefore proposed. Both approaches require four temperature measurements: t_s, t'_s, t_e, t'_e.

5.1.1 Performance curves approach

Heat transfer efficiency (η) is a widely-used parameter for characterizing a recuperator. It depends on the physical parameters of the recuperator, the air flow rates and the humidity [65] and can be expressed by performance curves. There is an empirically established dependency $\eta = f(\dot{m})$, where $\dot{m}$ is the mass flow rate of the fluid of interest (kg/s). Performance curves are usually provided by the manufacturer in the form of a graph.

The efficiency of the heat transfer of the recuperator is expressed as [65, 46]:

$$\eta = \frac{Q}{Q_{max}} = \vartheta_s \frac{\dot{C}_s}{\dot{C}_{min}} = \vartheta_e \frac{\dot{C}_e}{\dot{C}_{min}} = \vartheta_{max}, \tag{5.1}$$

where $\dot{C}$ is the heat capacity rate of the fluid (W/K), $\dot{C}_{min}$ is the minimum of $\dot{C}_s$ and $\dot{C}_e$ (index s is used for the supply flow and index e is used for the exhaust flow), $Q(Q_{max})$ is the heat flow (W), ϑ_{max} is the maximum value of ϑ_s and ϑ_e. The ϑ is the temperature ratio calculated as [65]:

$$\vartheta_s = \frac{t'_s - t_s}{t_e - t_s}, \tag{5.2}$$

$$\vartheta_e = \frac{t'_e - t_e}{t_e - t_s}, \tag{5.3}$$

where all temperatures are expressed in (^{o}C). If the heat capacity rate of the flow is substituted by equation [65]:

$$\dot{C} = c \cdot \dot{m} = V \cdot \rho \cdot c, \tag{5.4}$$

where c is the specific heat of the fluid (J/(kg·K) (c can be considered as constant within the temperature and pressure ranges typical of AHUs: -40 to $40\,^{\circ}$C, atmospheric pressure about 101kPa), $\dot{m}$ is the mass flow rate (kg/s), V is the air flow rate (m^3/s), ρ is the air density (kg/m^3), equation (5.1) can be modified as follows [65]:

$$\eta = \vartheta_s \frac{\dot{m}_s}{\dot{m}_{min}} = \vartheta_e \frac{\dot{m}_e}{\dot{m}_{min}} = \vartheta_{max}. \tag{5.5}$$

According to equation (5.5) and known dependency described by the performance curve, the following formulas can be derived: for $\vartheta_s \geq \vartheta_e \Rightarrow \vartheta_{max} = \vartheta_s$, ($\dot{m}_s \leq \dot{m}_e$):

$$\dot{m}_s = f^{-1}(\vartheta_s), \dot{m}_e = \dot{m}_s \frac{\vartheta_s}{\vartheta_e}, \tag{5.6}$$

and for $\vartheta_s < \vartheta_e \Rightarrow \vartheta_{max} = \vartheta_e$, $(\dot{m}_s > \dot{m}_e)$:

$$\dot{m}_s = \dot{m}_e \frac{\vartheta_e}{\vartheta_s}, \dot{m}_e = f^{-1}(\vartheta_e). \tag{5.7}$$

where $\dot{m}_s$ is the mass flow of the supply air, $\dot{m}_e$ is the mass flow of exhaust air and f is a polynomial function describing dependency between heat transfer efficiency and mass flow rate ($\eta = f(\dot{m})$). This dependency is expressed by the performance curve. In a case, that the performance curve is not available, it can be measured (see section 5.3.5). The performance curve has been measured and calculated according to the following equation:

$$\eta = \frac{V_s \cdot \rho_s \cdot (t'_s - t_s)}{\min(V_e \cdot \rho_e, V_s \cdot \rho_s) \cdot (t_e - t_s)}. \tag{5.8}$$

where V_s is the supply air flow rate, V_e is the exhaust air flow rate, ρ_s is the supply air density and ρ_e is the exhaust air density.

5.1.2 Recuperator geometry approach

The energy exchange process in the recuperator can be modeled as the heat transfer between two fluids flowing through a flat plate. A mathematical model of this process is derived taking into account certain simplifications:

1. A recuperator is considered as a single rectangular plate which represents a surface for heat transfer.
2. The flow arrangement is countercurrent.
3. Heat losses are neglected.
4. The heat transfer process is steady-state.

The heat exchange process is considered as quasi-static, $\dot{Q}$ amount of heat is transferred between $\dot{m}_s$ of supply air and $\dot{m}_e$ of exhaust air. As a result, the temperatures of the supply and exhaust air change respectively from t_s to t'_s and from t_e to t'_e (see Fig. 5.2). The image 5.2 shows the heat exchange process in a recuperator,- where $\dot{m}_s$ is the mass flow of

the supply air $\dot{m}_e$ is the mass flow of the exhaust air, $t_s$is the temperature of the supply air at the inlet of the recuperator, t'_s is the temperature of the supply air at the outlet of the recuperator, t_e is the temperature of the exhaust air at the inlet of the recuperator, and t'_e is the temperature of the exhaust air at the outlet of the recuperator, $\dot{Q}$ is the transferred heat, and S is the surface between two plates.

Generally, the heat received by matter causes a change in the temperature of the matter according to the heat equation [65]:

$$\dot{Q} = \dot{m} c_p \Delta T, \tag{5.9}$$

where $\dot{Q}$ is the transferred heat (W), and ΔT is the change in temperature (K).

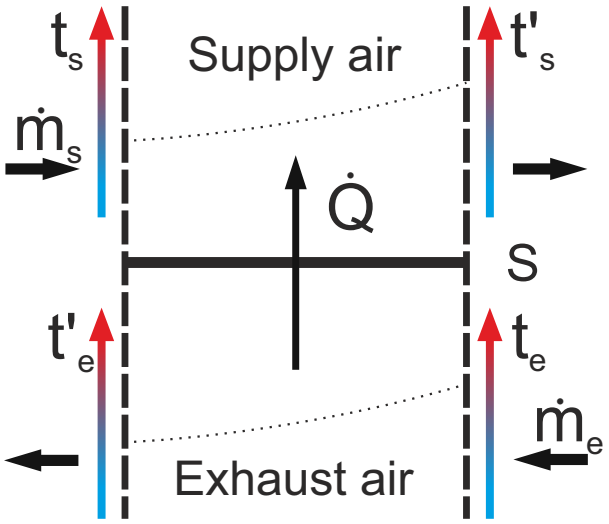

Figure 5.2: The heat exchange process in a recuperator.

However, the heat transfer between two fluids in a counter-current recuperator (convection - conduction - convection mechanism) is:

$$\dot{Q}' = x \Delta T_m, \tag{5.10}$$

where ΔT_m is the logarithmic mean temperature difference (LMTD) [65]:

$$\Delta T_m = \frac{(t_e - t'_s) - (t'_e - t_s)}{ln(\frac{t_e - t'_s}{t'_e - t_s})}, \tag{5.11}$$

and

$$x = \frac{S}{\frac{1}{h_s} + \frac{\delta}{\lambda_p} + \frac{1}{h_e}}, \tag{5.12}$$

where δ is the thickness of plate (m), λ_p is the thermal conductivity of plate ($Wm^{-1}K^{-1}$), h_s and h_e are the heat transfer coefficients on the supply and exhaust sides of the plates ($W/(m^2K)$) and S is the equivalent heat transfer surface (m^2).

Equations are derived for the counter-current arrangement of the flows. For cross-current heat exchangers, the formula for LMTD should be corrected by coefficient F [30]:

$$\Delta T_m, corr = F\Delta T_m, \tag{5.13}$$

where coefficient F< 1 depends on the type of exchanger and the flow rate ratio [65].

The heat transfer coefficients depend on the flow regime, the characteristics of the fluid, the plate dimensions and for the case of airflow around the plate it can be described as [30]:

$$h = \frac{Nu\lambda_f}{L}, \tag{5.14}$$

where Nu is the Nusselt number (the dimensionless average heat transfer rate), λ_f is the thermal conductivity of a fluid ($Wm^{-1}K^{-1}$), L - characteristic linear dimension (m), which for rectangular duct is calculated as the hydraulic diameter:

$$L = D_h = \frac{2a_p h_p}{a_p + h_p}. \tag{5.15}$$

where a_p and h_p are dimensions of a plate (see Fig. 5.3). The Nusselt number is generally a function of the Reynolds number and the Prandtl number. The exact form of the equation is geometry-specific, and is derived empirically for each case [61].

The average Nusselt number over a flat plate for the laminar regime is [30]:

$$Nu^* = 0.664 Re^{0.5} Pr^{1/3}, \tag{5.16}$$

and for turbulent flow:

$$Nu^* = 0.035Re^{0.8}Pr^{1/3} \tag{5.17}$$

where Re is the Reynolds number [30] and Pr is the Prandtl number [30]:

$$Re = \frac{uL}{\nu}, \tag{5.18}$$

$$Pr = \frac{\nu}{\alpha}, \tag{5.19}$$

where u is the flow velocity (m/s), ν is the kinematic viscosity of the fluid (m^2/s) and α is the thermal diffusivity of the fluid (m^2/s).

The mean flow velocity u inside the recuperator can be calculated from the mass flow rate $\dot{m}$ with the equation:

$$\dot{u} = \frac{\dot{m}}{nS_c\rho} = \frac{\dot{m}}{n \cdot a_p \cdot h_p \cdot \rho}, \tag{5.20}$$

where S_c is the area of a single channel between two plates(m^2), ρ is the air density (kg/m^3) and n is the number of channels.

Since the plates of a recuperator are usually equipped with fins, a correction should be made for fin efficiency η:

$$Nu = \eta Nu^*. \tag{5.21}$$

Equation for triangular fin efficiency:

$$\eta = \frac{tanh\sqrt{0.5Nu^*\frac{\lambda_f}{\lambda_p}\frac{l_p}{D_h}\frac{l_p}{\delta}(\frac{\delta}{b_p}+1)}}{\sqrt{0.5Nu^*\frac{\lambda_f}{\lambda_p}\frac{l_p}{D_h}\frac{l_p}{\delta}(\frac{\delta}{b_p}+1)}}, \tag{5.22}$$

where b_p,l_p,δ are the dimensions of the plate according to Fig. 5.3.

From the assumption that the supply air is colder:

$$\dot{Q}_s = \dot{Q}_e = \dot{Q}', \tag{5.23}$$

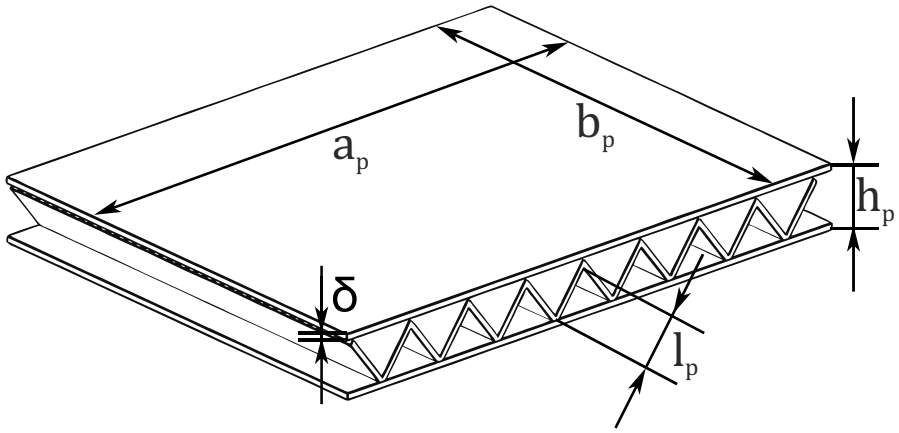

Figure 5.3: Plate geometry

$$\dot{m}_s \cdot c_{ps}(t'_s - t_s) = \dot{m}_e \cdot c_{pe}(t_e - t'_e) = x\Delta T_m, \tag{5.24}$$

consequently the mass flow of the supply air is:

$$\dot{m}_s = \frac{\Delta T_m}{t'_s - t_s} \cdot \frac{x}{c_{ps}}, \tag{5.25}$$

and the mass flow of the exhaust air is:

$$\dot{m}_e = \frac{\Delta T_m}{t'_e - t_e} \cdot \frac{x}{c_{pe}}. \tag{5.26}$$

Quantities ρ,λ,ν and c_p in equations (5.10)-(5.26) depend on temperature. Their values are calculated based on linear interpolation of characteristic properties of air at the temperature which is established as a mean value between the temperature at the inlet and outlet of the recuperator. These quantities are calculated for each flow separately. Also, quantities ρ,λ,ν and c_p are dependent on air pressure and humidity. All air in an open system is under atmospheric pressure, which is about 101kPa. The temperature range of the recuperator for a typical AHU is within the range of -40 to $40\,^{\circ}$C. The influence of pressure and humidity is not significant at these ranges [68]. This dependency has been neglected, due to lack of the respective sensors in commercial AHUs, and because the impact of pressure and humidity is much lower than the impact of temperature.

Condensation or frost inside the recuperator dramatically changes the heat transfer process, which significantly complicates the calculations. However, with properly operating anti-freeze protection and average humidity of the indoor air, these states should not occur during AHU operation.

5.2 Recuperator parameters in BIM

The IFC BIM contains two basic entities for definition of recuperator. This device can be represented by the *IfcAirToAirHeatRecovery* entity, or recuperator can be defined by *IfcAirToAirHeatRecoveryType* and connected by *IfcRelDefinesByType* to *IfcAirToAirHeatRecovery*. *IfcAirToAirHeatRecovery* entity is part of the group *IfcEnergyConversionDevice* that further comprises, for example boiler, chiller, coil, cooling tower or electric generator. The parent objects are *IfcDistributionFlowElement*, *IfcElement*, *IfcProduct* and the highest object is *IfcObject*. Example of IFC air to air heat recovery entity in XML specification:

```
<?xml version="1.0"?>
<ConceptRoot xmlns:xsi="http://www.w3.org/2001/XMLSchema-instance"
xmlns:xsd="http://www.w3.org/2001/XMLSchema"
uuid="4547fced-b3cc-41b8-ae65-87d2d78fdd38"
name="IfcAirToAirHeatRecovery"
status="sample"
applicableRootEntity="IfcAirToAirHeatRecovery">
  <Applicability uuid="00000000-0000-0000-0000-000000000000" status="sample">
    <Template ref="ec91f9a5-286c-429c-a311-bb64d3bf709a" />
    <TemplateRules operator="and" />
  </Applicability>
  <Concepts>
    <Concept uuid="dca01def-c6e7-4875-af10-ef6032ad9017"
    name="Object Typing" status="sample" override="false">
      <Template ref="35a2e10e-20df-40f4-ab2f-dacf0a6744f4" />
      <TemplateRules operator="and">
        <TemplateRule Parameters="RelatingType[Type]='IfcAirToAirHeatRecoveryType'" />
      </TemplateRules>
    </Concept>
    <Concept uuid="05c1d841-8b23-469c-b4ad-50c491d7f0d2"
    name="Property Sets for Objects" status="sample" override="false">
      <Template ref="f74255a6-0c0e-4f31-84ad-24981db62461" />
      <TemplateRules operator="and">
        <TemplateRule Parameters="PsetName[Value]='Pset_AirToAirHeatRecoveryTypeCommon'" />
      </TemplateRules>
    </Concept>
    <Concept uuid="2b8c854a-2df2-46e2-be51-c3401be67a63"
    name="Quantity Sets" status="sample" override="false">
      <Template ref="6652398e-6579-4460-8cb4-26295acfacc7" />
      <TemplateRules operator="and">
        <TemplateRule Parameters="QsetName[Value]='Qto_AirToAirHeatRecoveryBaseQuantities'" />
```

```
32        </TemplateRules>
33      </Concept>
34      <Concept uuid="f6e94660-bf0c-4989-8442-39782f2a1dfb"
35      name="Material" status="sample" override="false">
36        <Template ref="d96f7f7d-e742-4db8-9b5d-18a36a6df884" />
37        <TemplateRules operator="and">
38          <TemplateRule Description="Material from which the casing is constructed."
39          Parameters="" />
40          <TemplateRule Description="The primary media material used for heat transfer."
41          Parameters="" />
42        </TemplateRules>
43      </Concept>
44      <Concept uuid="69f6df9c-5d01-4d71-a8c5-a70e465acf06"
45      name="Port" status="sample" override="false">
46        <Template ref="bafc93b7-d0e2-42d8-84cf-5da20ee1480a" />
47        <TemplateRules operator="and">
48          <TemplateRule Description="Conditioned air in."
49          Parameters="PortName[Value]='AirInlet'
50          AND SystemType[Value]='AIRCONDITIONING' AND Flow[Value]='SINK'" />
51          <TemplateRule Description="Conditioned air out."
52          Parameters="PortName[Value]='AirOutlet'
53          AND SystemType[Value]='AIRCONDITIONING' AND Flow[Value]='SOURCE'" />
54          <TemplateRule Description="Exhausted air in."
55          Parameters="PortName[Value]='ExhaustInlet'
56          AND SystemType[Value]='AIRCONDITIONING' AND Flow[Value]='SINK'" />
57          <TemplateRule Description="Exhausted air out."
58          Parameters="PortName[Value]='ExhaustOutlet'
59          AND SystemType[Value]='AIRCONDITIONING' AND Flow[Value]='SOURCE'" />
60        </TemplateRules>
61      </Concept>
62    </Concepts>
63  </ConceptRoot>
```

Definition of *IfcAirToAirHeatRecovery*: An air-to-air heat recovery device employs a counter-flow heat exchanger between inbound and outbound air flow. It is typically used to transfer heat from warmer air in one chamber to cooler air in the second chamber, resulting in energy savings from reduced heating (or cooling) requirements [39].

The energy conversion device type *IfcAirToAirHeatRecoveryType* defines the information of air to air heat recovery. The set of information may include [39]:

- common properties with shared property sets
- common representations
- common materials
- common composition of elements

Constant	Description
FIXEDPLATECOUNTER-FLOWEXCHANGER	Heat exchanger with moving parts and alternate layers of plates, separated and sealed from the exhaust and supply air stream passages with primary air entering at secondary air outlet location and exiting at secondary air inlet location.
FIXEDPLATECROSSFL-OWEXCHANGER	Heat exchanger with moving parts and alternate layers of plates, separated and sealed from the exhaust and supply air stream passages with secondary air flow in the direction perpendicular to primary air flow.
FIXEDPLATEPARALLE-LFLOWEXCHANGER	Heat exchanger with moving parts and alternate layers of plates, separated and sealed from the exhaust and supply air stream passages with primary air entering at secondary air inlet location and exiting at secondary air outlet location.
ROTARYWHEEL	A heat wheel with a revolving cylinder filled with an air-permeable medium having a large internal surface area.
RUNAROUNDCOIL-LOOP	A typical coil energy recovery loop places extended surface, finned tube water coils in the supply and exhaust airstreams of a building.
HEATPIPE	A passive energy recovery device with a heat pipe divided into evaporator and condenser sections.
TWINTOWERENTHALPY-RECOVERYLOOPS	An air-to-liquid, liquid-to-air enthalpy recovery system with a sorbent liquid circulates continuously between supply and exhaust airstreams, alternately contacting both airstreams directly in contactor towers.
THERMOSIPHONSEALE-DTUBEHEATEXCHANGERS	Sealed systems that consist of an evaporator, a condenser, interconnecting piping, and an intermediate working fluid that is present in both liquid and vapor phases where the evaporator and the condenser are usually at opposite ends of a bundle of straight, individual thermosiphon tubes and the exhaust and supply ducts are adjacent to each other.
THERMOSIPHONCOILT-YPEHEATEXCHANGERS	Sealed systems that consist of an evaporator, a condenser, interconnecting piping, and an intermediate working fluid that is present in both liquid and vapor phases where the evaporator and condensor coils are installed independently in the ducts and are interconnected by the working fluid piping.
USERDEFINED	User-defined air to air heat recovery type.
NOTDEFINED	Undefined air to air heat recovery type.

Table 5.1: General types of air-to-air heat recovery devices

IfcAirToAirHeatRecoveryTypeEnum defines general types of air-to-air heat recovery devices. The applicable options are listed in Table 5.1.

Property sets are defined by *IfcPropertySet* and attached to an entity through the *IfcRelDefinesByProperties*. The list of all the parameters that can be used to specify a recuperator in IFC is given in tables 5.2 and 5.3. *IcAirToAirHeatRecovery* entity provides all information necessary for the virtual sensor based on the recuperator geometry approach. The virtual sensor based on the performance curves approach cannot be automatically configured by standard IFC BIM. The performance curve can be saved by recuperator

Name	Type	Description
Sensible-Effectiveness	*P_REFERENCEVALUE* *IfcTimeSeries* *IfcNormalisedRatioMeasure*	Sensible heat transfer effectiveness, where effectiveness is defined as the ratio of heat transfer to maximum possible heat transfer.
Total-Effectiveness	*P_REFERENCEVALUE* *IfcTimeSeries* *IfcNormalisedRatioMeasure*	Total heat transfer effectiveness: The ratio of heat transfer to the maximum possible heat transfer.
Temperature-Effectiveness	*P_REFERENCEVALUE* *IfcTimeSeries* *IfcNormalisedRatioMeasure*	Temperature heat transfer effectiveness: The ratio of primary airflow temp. changes to maximum possible temp. changes.
Defrost-Temperature-Effectiveness	*P_REFERENCEVALUE* *IfcTimeSeries* *IfcNormalisedRatioMeasure*	Temperature heat transfer effectiveness when defrosting is active.
Humidity-Effectiveness	*P_REFERENCEVALUE* *IfcTimeSeries* *IfcNormalisedRatioMeasure*	Humidity heat transfer effectiveness: The ratio of primary airflow absolute humidity changes to maximum possible absolute humidity changes.
Sensible-Heat-TransferRate	*P_REFERENCEVALUE* *IfcTimeSeries* *IfcPowerMeasure*	Sensible heat transfer rate.
LatentHeat-Transfer-Rate	*P_REFERENCEVALUE* *IfcTimeSeries* *IfcPowerMeasure*	Latent heat transfer rate.
TotalHeat-Transfer-Rate	*P_REFERENCEVALUE* *IfcTimeSeries* *IfcPowerMeasure*	Total heat transfer rate.
Sensible-Effectiveness-Table	*P_REFERENCEVALUE* *IfcTimeSeries*	Sensible heat transfer effectiveness curve as a function of the primary and secondary air flow rate.
Total-Effectiveness-Table	*P_REFERENCEVALUE* *IfcTimeSeries*	Total heat transfer effectiveness curve as a function of the primary and secondary air flow rate.
AirPressure-DropCurves	*P_REFERENCEVALUE* *IfcTimeSeries*	Air pressure drop as function of air flow rate.

Table 5.2: Properties of Air To Air Heat Recovery Part 1/2

manufacturer like *USERDEFINED* type of air-to-air heat recovery device.

5.3 Experimental AHU unit and laboratory tests

All of the laboratory tests were performed on an experimental AHU test rig (see Figure 5.4), which was designed for experimental validation of the performance monitoring and FDD (Fault Detection and Diagnostics) methods.

Name	Type	Description
Reference	*P_SINGLEVALUE IfcIdentifier*	Reference ID for this specified type in this project.
Status	*P_ENUMERATEDVALUE IfcLabel PEnum_ElementStatus*	Status of the element, predominately used in renovation or retrofitting projects.
Heat Transfer Type Enum	*P_ENUMERATEDVALUE IfcLabel PEnum_AirToAirHeat-TransferHeatTransferType*	Type of heat transfer between the two air streams.
Has Defrost	*P_SINGLEVALUE IfcBoolean*	Has the heat exchanger has defrost function or not.
Operational Temperature Range	*P_BOUNDEDVALUE IfcThermodynamic-TemperatureMeasure*	Allowable operation ambient air temperature range.
Primary Airflow Rate Range	*P_BOUNDEDVALUE IfcVolumetricFlow-RateMeasure*	Possible range of primary airflow that can be delivered..
Secondary Airflow Rate Range	*P_BOUNDEDVALUE IfcPressureMeasure*	Possible range of secondary airflow that can be delivered.

Table 5.3: Properties of Air To Air Heat Recovery Part 2/2

5.3.1 Experimental HVAC unit

The goal of this chapter is to introduce a unique system for research and development of new FDD methods and new virtual sensors. We developed experimental HVAC system designed for data collection and its further processing. The individual sensors with their parameters and data logger will be introduced in this part.

The primary objective of the developed experimental HVAC unit system is to identify conditions of air flow through the unit at any spots where the variations can be measured. These spots include obstacles e.g. filter, fan... or when air flow passes from one chamber to another. Furthermore, the energy consumption of the fully operational air conditioning is measured. Fig.5.5. shows a block diagram with new sensors of the HVAC unit.

5.3.2 Technical description of the test rig

Principal measured parameters are air temperature, humidity and the dew point. In addition, air velocity and differential pressures are measured. Many other values are subsequently calculated such as air flow rate, specific air humidity, specific enthalpy, specific density, heat recovery efficiency, thermal output of heater/cooler, effective humidification,

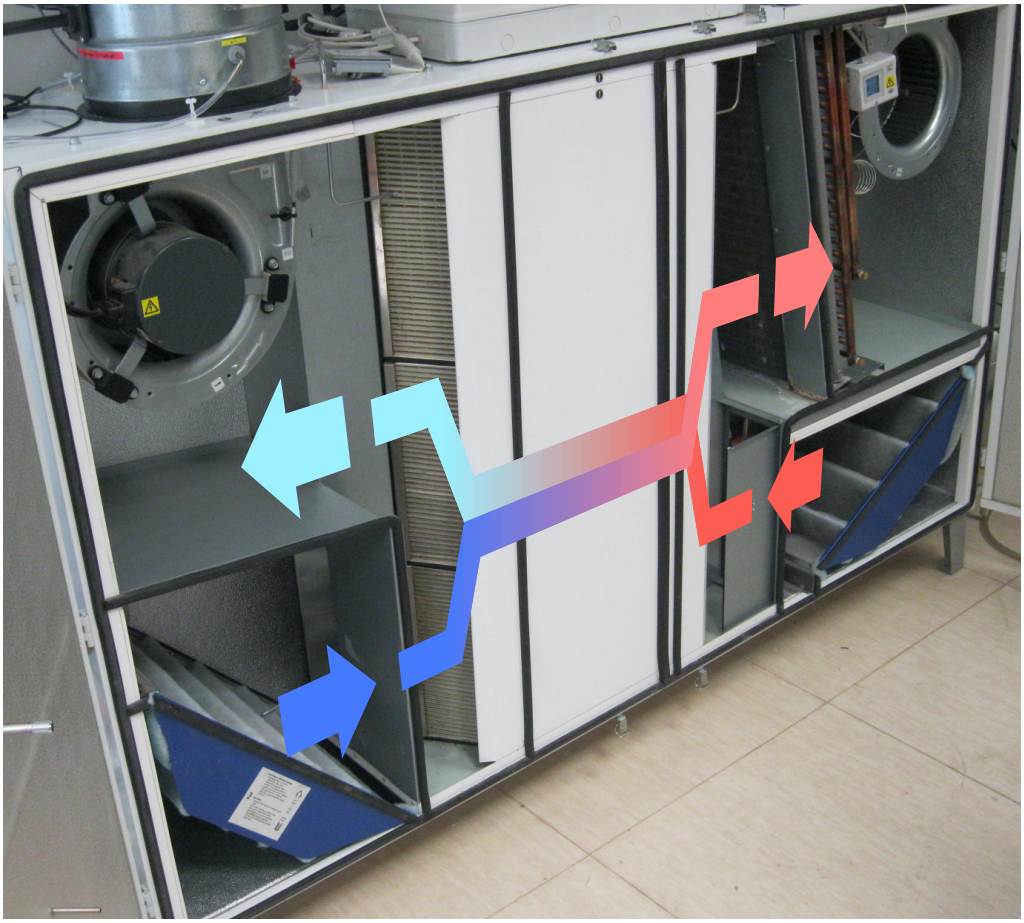

Figure 5.4: General view of an open AHU with the recuperator highlighted

fan air temperature increase and fan thermal output. Heat/cold consumption, water consumption and electric energy consumption are measured from energy consumption. A diagram of sensors is displayed in Fig.5.6.

5.3.2.1 Sensors

A list of sensors is summarized in Table 5.4. The temperature measurement, relative humidity and dew point are integrated into one sensor. The temperature is measured using thermistor Pt1000. For the air velocity measurement a turbine flow meter is used.

All the consumption energy meters are instruments designated for household use, and as such they are not suitable for laboratory purposes (they are typically used for remote reading of consumed energy). In an experimental HVAC system two heat/cold consumption meters are used: Landis+Gyr ULTRAHEAT/ COLD T230. The Sensors measure

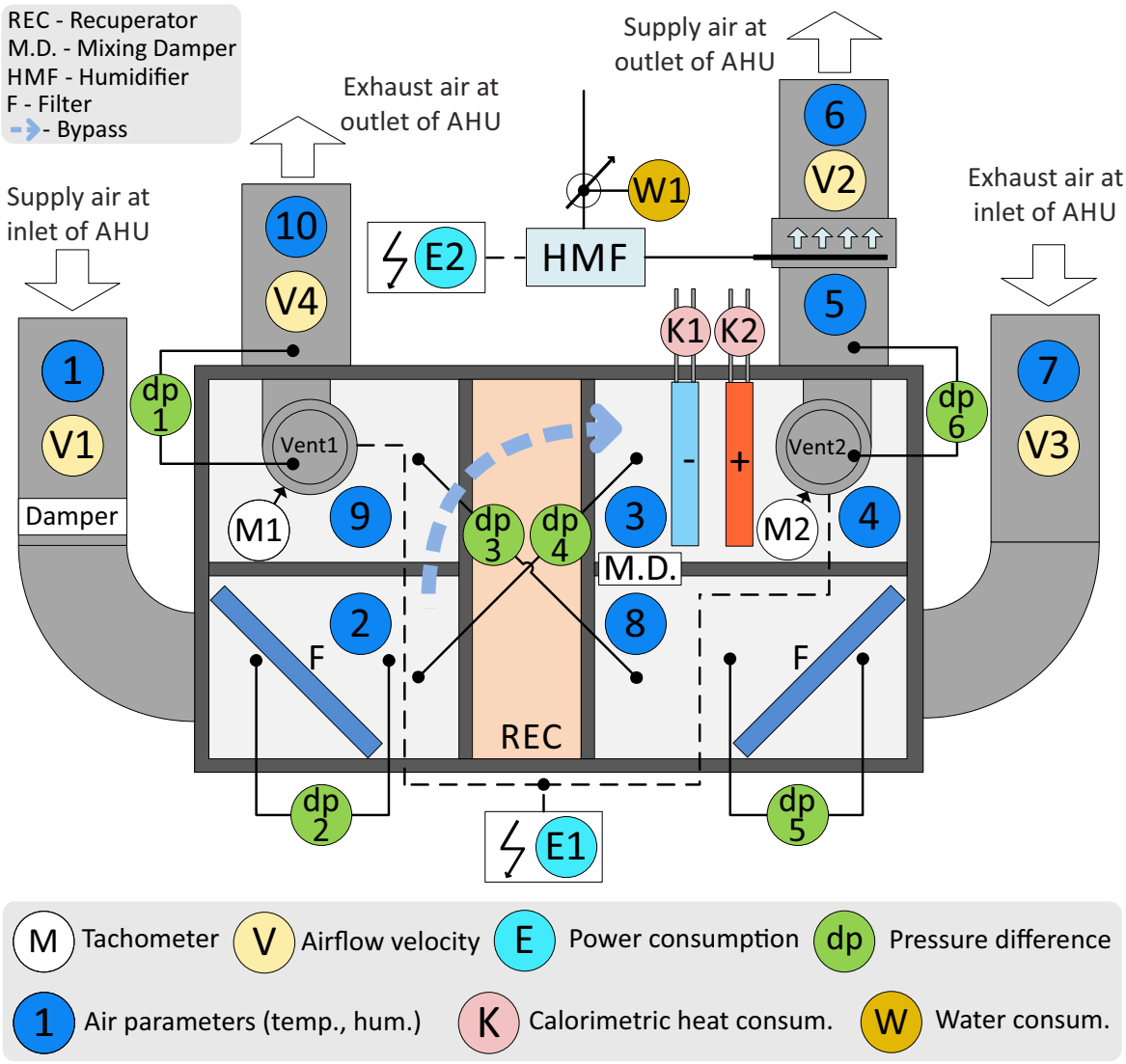

Figure 5.5: Block arrangement of the AHU test rig.

temperature of a liquid at the input and output and there is also an ultrasound measurement of flow. The heat/cold consumption is calculated based on measured values with a measurement error less than 2%. The working range of temperature is 5 - 90°C and the maximum rate of flow is 5m^3/h. The consumption of heat/cold is displayed on LCD in kWh (MWh) or kJ (MJ) and at the same time the device allows to export all measured data using M-bus. Electronic water meter Siemens - WFC21.E130 with metrology accuracy - B is used for the measurement of water consumption of the humidifier. This means that it allows to measure flow with minimum rate of 30l/h and with accuracy ±5%. The temperature of water has to be less than 30°C and the nominal flow rate should be around 2,5m^3/h. The device displays measured consumption of a liquid on LCD and exports measured data using M-Bus. The electric meters used for measuring electric energy

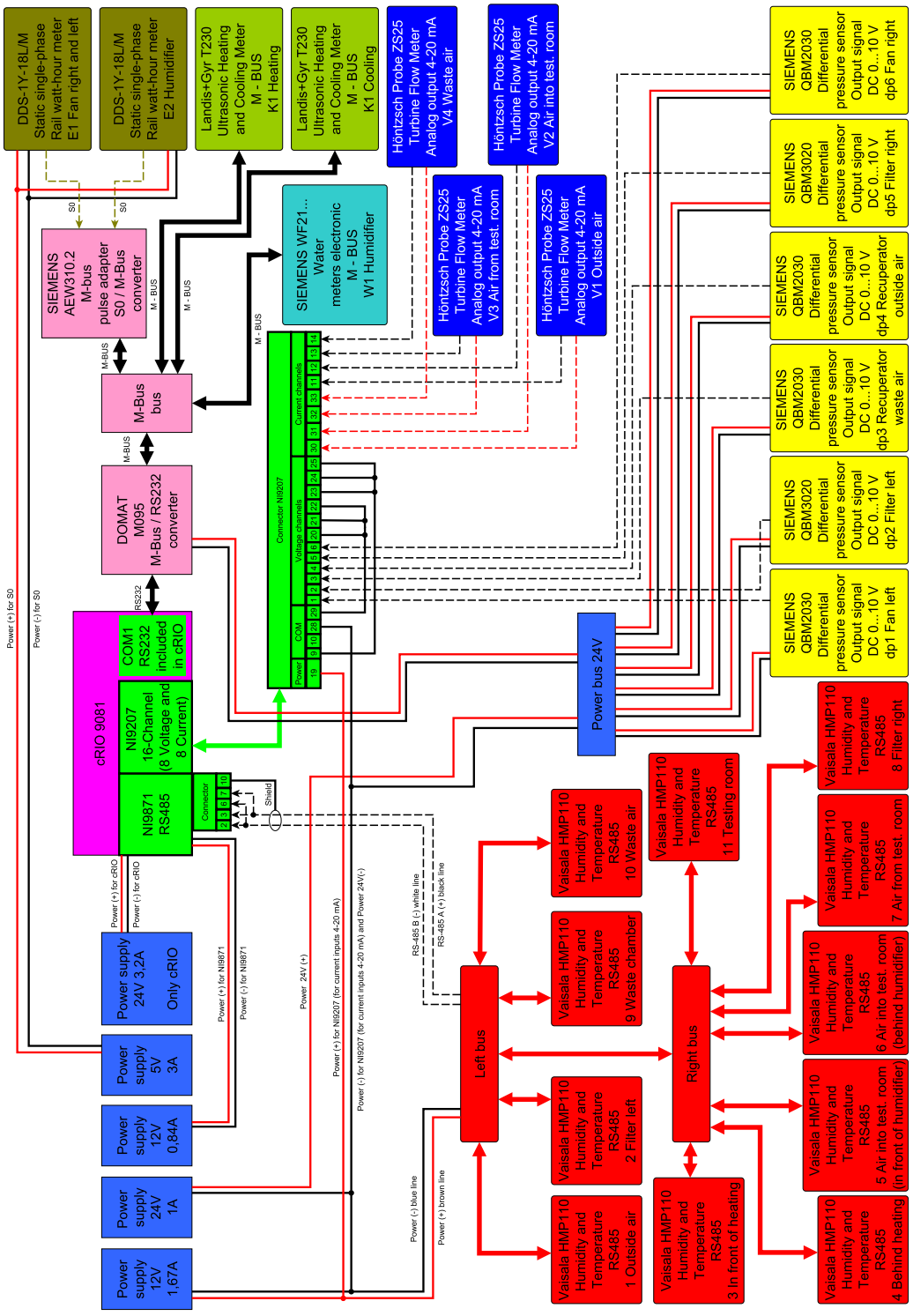

Figure 5.6: Circuit diagram of all new sensors used for AHU monitoring

Sensor	Measured range	Accuracy	Color in Figure
Temperature	0 to +40°C -40 to 0°C +40 to +80°C	±0,2°C ±0,4°C ±0,4°C	Red
Relative humidity	0 to 90% 90 to 100%	±1,7% RH ±2,5% RH	Red
Flow meter	0-20m/s	1.5% of value +0.5% of full range	Blue
Differential pressure *Fans* *Filters* *Heat exchanger*	 0-1000Pa 0-300Pa 0-200Pa	 ±3% of full-range ±0.7% of full-range ±3% of full-range	Yellow

Table 5.4: List of sensors

consumption are DDS-1Y-18L/M. They are single phase electric meters with maximum measurement error 1% and pulse outputs. The output of the electric meter constitutes a solid-state relay which generates pulses each time when 1Wh is consumed. The duration of one pulse is 90ms and the voltage of the pulses depends on the pulse adapter. Electric meters are connected to the pulse adapter (Siemens AEW310.2), which communicates using M-Bus. Electric meters display current values of consumed energy on LCDs.

5.3.2.2 Logger

The basic unit of the measuring system is IN CompactRIO 9081. It is fully-fledged industrial computer with the ability to connect different measuring modules, which collects processes and stores all measured data. NI CompactRIO - 9081 runs with an industrial version of the operating system Windows - Windows Embedded 7 and it is programmed with NI LabVIEW graphical programming tools. In this project two cRIO modules are used - NI 9871 and NI 9207. NI 9871 consists of 4 independent RS-485 (RS-422) ports where each port can handle up to 32 RS485-based devices. NI 9207 allows connection of up to 8 voltage-output devices and up to 8 current loop devices. Measuring ranges are ±10V and ±21,25mA with 24-bit resolution, which means that the quantization step is 0,6μV and 1,3nA. The sampling rate is 500 samples per second (high-speed mode) per all channels which means 30 samples per channel. M-Bus an RS-232 port is used for communication, which is directly on cRIO and RS-232/M-Bus converter. These four interfaces (RS-485, voltage-output, current loop and M-Bus) provide a basic access to all of used sensors and devices.

For data processing a program in LabVIEW was created. When the measuring process starts, the program collects data from the sensors on RS-485 (measuring the conditions of the air), then it collects all data from sensors connected to the module which measures

analog values (air flow rate and differences of pressures). In the next step the program collects data from an OPC server from sensors connected to the M-Bus and finally it calculates the rest of the values from the collected data. It takes about 4 seconds to collect one set of data depending on the speed of the communication via RS-485 interface. Data from the M-Bus are ensured by Runtime program to run in the background as a service and sends the resulting data to the OPC server. Every single set of data measured in one cycle is displayed on a diagram of the HVAC system and several values are plotted in graphs. The last set of collected data are stored regularly. This time period can be set. These stored data can be used for further processing.

Figure 5.7: General view of AHU with new sensors

5.3.3 Purpose of test rig

HVAC unit is connected to a special testing chamber where various conditions can be set thanks to the possibility to heat or cool each wall separately. On the HVAC system a lot of disturbances typical for HVAC units (like clogged filter etc.) can be simulated. Thanks to monitoring of the system and processing of stored data, new FDD methods will be developed. These methods, which were obtained from our unit (photos of our system are in Fig.5.7. and 5.8.), can be used for more efficient and economical usage of other HVAC units. The system developed from us enables tested published FDD methods, which only on simulated data was tested. Our system will be used for virtual sensors testing.

For example, faults for regarding the air intake process can be simulated. These faults do not cause a loss of comfort and remain undetected for HVAC controlling devices. This

Figure 5.8: General view of an open AHU

results in an increase in energy consumption of HVAC and therefore it increases HVAC costs.

5.3.3.1 Fault of outside air damper - mode circulation

Fault simulates seizure of outside air damper [69]. Outside air damper is permanently open. The system is OK for mode without circulation. The circulation mode needs outside air damper closed and seizure of damper can induce increase in energy consumption of heating or cooling. Curves in Figure 5.9. describe the following three operational modes of HVAC:

- time from 18.1 to 18.25 - mode without circulation, HVAC without fault
- time from 18.25 to 18.34 - mode circulation, HVAC without fault
- time from 18.34 to 18.45 - mode circulation, HVAC with fault of outside air damper

HVAC controller in circulation mode (HVAC without fault) turns off a return fan and closes outside air damper. Air flows only from testing room and supply fan have to increase the power (supply fan maintains steady-state flow V2). If the outside air damper is open, the power of supply fan will be lower. From here air flows from the testing room and from the outside. The supply fan reduces power for maintained steady-state flow V2.

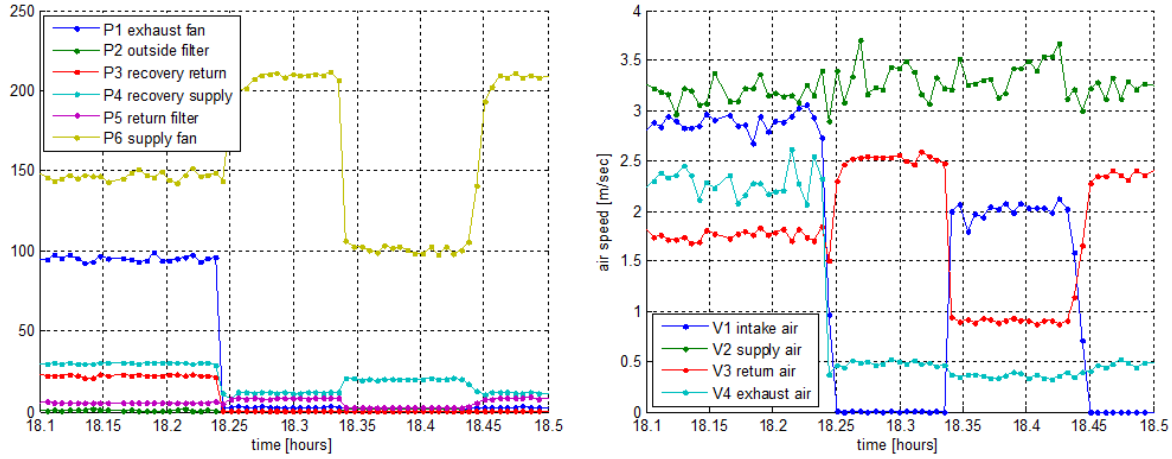

Figure 5.9: Simulation of fault of outside air damper, differential pressure (left graph) and air velocity (right graph)

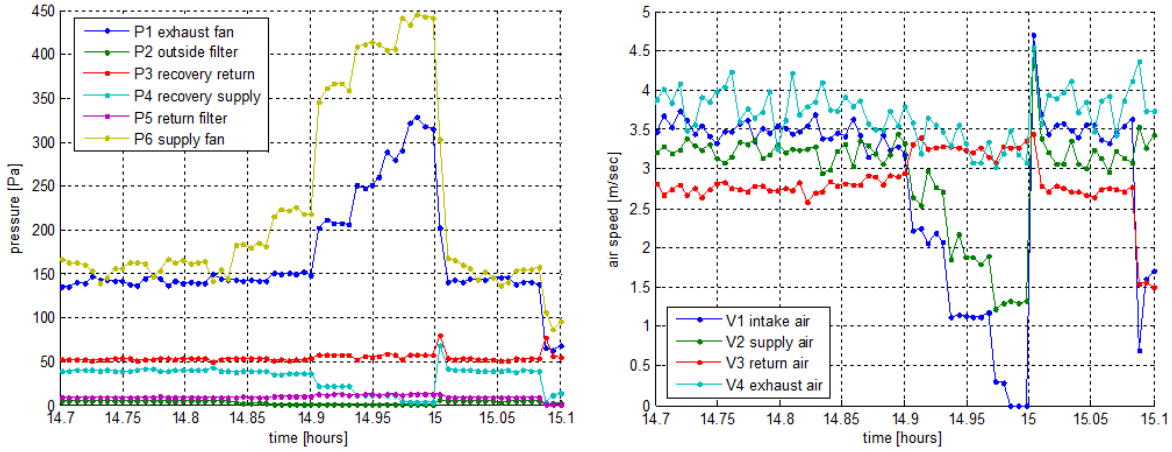

Figure 5.10: The simulation of fault of fouling process for exterior louver, differential pressure (left graph) and air velocity (right graph)

5.3.3.2 Fouling process for exterior louver

The intake pipe may be clogged with leaves, or by other kind of impurities. Measured differential pressures and air velocities are depictured in Figure 5.10. Simulation of fault was made by outside air damper. Every two minutes (0.033 hours in Figure 5.10) the position of the damper was changed. From fully open (0°=0%) to close (90°=100%), one increment of the swing is 9°=10%. The power of the fans was not changed for angles in range from 0% to 60%. From 70% (14.9 hours in Figure 5.10) the power of the supply fan was increased but the air flow was not changed. The increase in energy consumption of the "supply fan" was undetected by the control system and it is a case of a latent fault. From

80% (14.83 hours in Figure 5.10) air flow to the test room was changed and fault can be detected by user.

Both of the above mentioned faults are characterized by an increase in operational cost of the HVAC system. Both of the faults can be detected by monitoring of differential pressure of "supply fan". It follows that sensor of differential pressure of "supply fan" is needed for FDD. However, a lot of common HVAC systems do not include this sensor. Therefore a virtual sensor is suitable as a substitution of a differential pressure sensor of "supply fan". The virtual sensor may work with history of electric energy consumption of a fan and with knowledge of the HVAC mode.

5.3.4 Laboratory experiments

Outputs of the proposed Virtual Sensor were compared with readings from V1 anemometers (Supply Air) and V4 anemometers (Exhaust Air) during laboratory tests. The measuring system provides a real-time calculation of the volumetric airflow from flow velocity measurements. Temperatures were measured by 4 sensors (see Fig. 5.5):

- Sensor 2 - Supply air at the inlet of the recuperator
- Sensor 3 - Supply air at the outlet of the recuperator
- Sensor 8 - Exhaust air at the inlet of the recuperator
- Sensor 9 - Exhaust air at the outlet of the recuperator

All measurements were conducted with a sampling rate of 12 seconds. The volumetric flow was converted to mass flow using data from multi-functional sensors 6 and 1 (Fig. 5.5 at the inlet and the outlet of the recuperator). The sensors provide information about temperature ($\pm 0.4\,^{\circ}\mathrm{C}$) and humidity ($\pm 2.5\% RH$) which were used to estimate the local air density inside the recuperator.

The experiments were executed on the AHU unit with a recuperator having the following parameters: Equivalent heat transfer surface: $98 m^2$. Single gap dimensions (see Fig. 5.3.): a_p=0.30m, b_p=0.50m, h_p=0.004m, δ=0.001m, l_p=0.006m. The number of gaps (in one direction) was 122. The thermal conductivity of the plate was $0.16 W m^{-1} K^{-1}$, and it was made of high impact polystyrene.

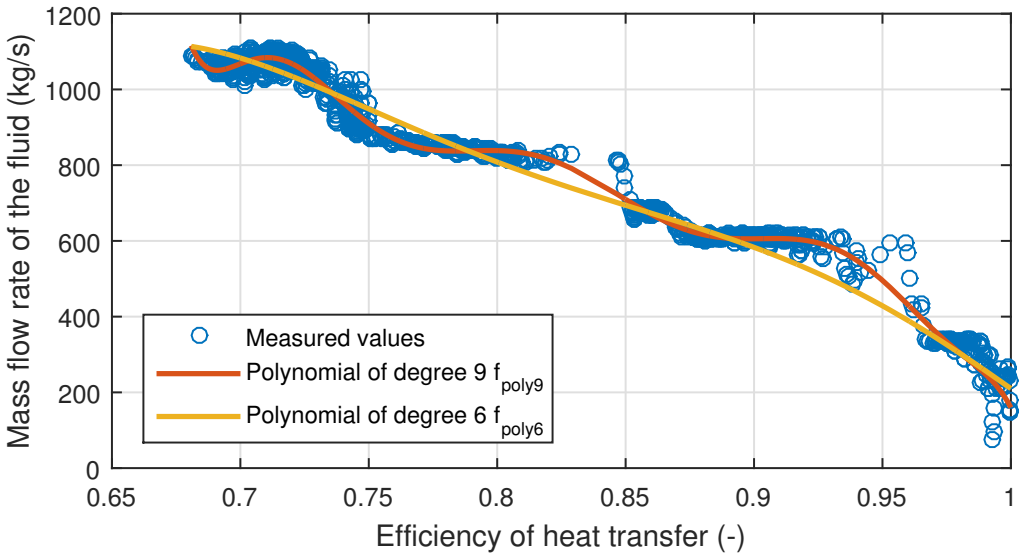

Figure 5.11: Performance curve of the test rig.

5.3.5 Performance curve measurement

The dependence of heat transfer efficiency on the mass flow rate of the fluid has been measured and calculated using equation 5.8, and it is described in Fig. 5.11.

Two polynomials have been tested to examine the sensitivity of the virtual sensor. The final value of $\dot{m}$ is determined by approximation curves. Approximation curves are described with a polynomial curve of degree 6 and 9 with the rounded coefficients shown in Table 5.5.

5.3.6 Transient state correction

The temperatures inside the recuperator have a long settling time (up to 20 minutes, depending on conditions). A model could potentially lose its accuracy during that period, due to violation of the steady-state assumption. This was confirmed by a laboratory test (see Fig. 5.12) in which the inlet damper position was changed every 10-15 min. This caused step-like flow changes of the supply air. The angle of the inlet damper is illustrated in the figures.

In order to improve the dynamic behavior of the performance curve model, equations (5.2) and (5.3) were corrected in the following way:

Constant	$poly_9$	$poly_6$
p_0	$2.1917 \cdot 10^{10}$	0
p_1	$-2.3779 \cdot 10^{11}$	-619660
p_2	$1.1437 \cdot 10^{12}$	3719579
p_3	$-3.2011 \cdot 10^{12}$	-8811101
p_4	$5.7452 \cdot 10^{12}$	10337412
p_5	$-6.8574 \cdot 10^{12}$	-6015491
p_6	$5.4431 \cdot 10^{12}$	1389471
p_7	$-2.771 \cdot 10^{12}$	-
p_8	$8.2074 \cdot 10^{11}$	-
p_9	$-1.078 \cdot 10^{11}$	-

Table 5.5: Polynomial coefficients

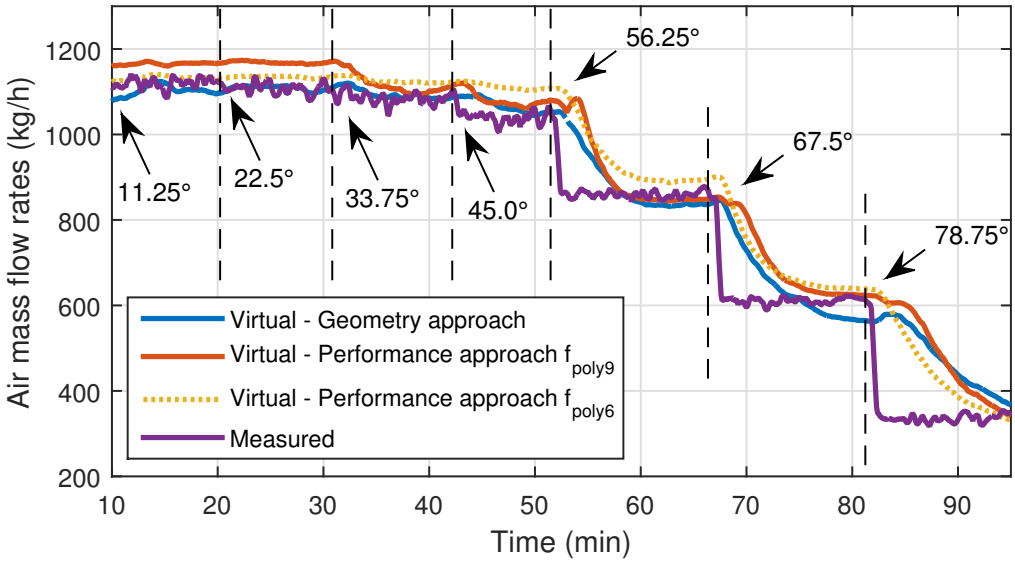

Figure 5.12: Supply mass airflow temperature settling

$$\vartheta'_s = \vartheta_s \cdot (1 + k_1 \frac{d\vartheta_s}{dt}), \vartheta'_e = \vartheta_e \cdot (1 + k_2 \frac{d\vartheta_e}{dt}), \tag{5.27}$$

where ϑ'_s and ϑ'_e are the corrected values of ϑ_s and ϑ_e and k_1 and k_2 are gain coefficients estimated empirically.

In addition, equations (5.25) and (5.26) for the geometry based model were improved:

$$\dot{m}'_s = \dot{m}_s \cdot (1 + k_3 \frac{d(\vartheta_e/\vartheta_s)}{dt}), \tag{5.28}$$

$$\dot{m}'_e = \dot{m}_s \cdot (1 + k_4 \frac{d(\vartheta_e/\vartheta_s)}{dt}), \tag{5.29}$$

where $\dot{m}'_s$ and $\dot{m}'_e$ are the corrected values of the air flow rates, and k_3 and k_4 are the empirically-estimated gain coefficients.

Additionally, outputs from all derivatives were filtered by SMA. Results of the tests with corrected models are presented in Fig. 5.13.

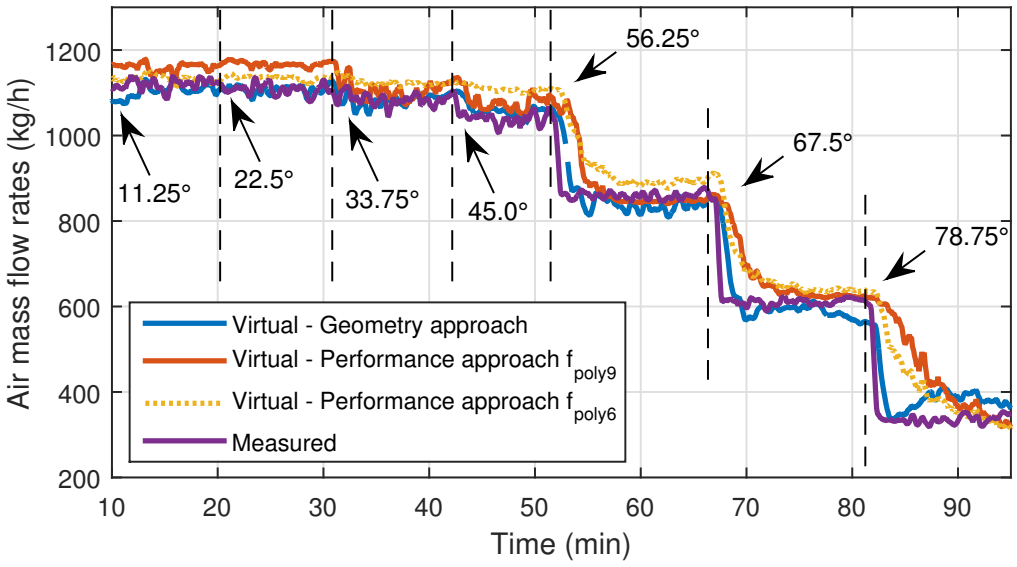

Figure 5.13: Supply mass airflow temperature settling, with corrections

Further VS testing was conducted with corrected models, as they provide a more accurate estimate for rapidly-changing conditions.

5.3.7 Laboratory test results

The tests were aimed to evaluate the performance of the models in conditions close to real-life operation, and to estimate possible weaknesses. The air mass flow rate based on the "Recuperator geometry approach" was calculated based on equations 5.6 and 5.7 and for "Performance curves approach" equations 5.25, 5.26 and two polynomial functions with different coefficients (see Tab. 5.5) were used.

Before the experiments started, the exhaust and supply fan speeds were set at maximum, the by-pass and circulation dumpers were set as closed, and the temperature inside the room (set-point) was set to $32°C$.

The main parameters were changed several times during the experiment: the fan speeds were set to different values (concurrently for both exhaust fans and supply fans, then independently); the temperature inside the room was gradually decreased until the heating was turned off completely. A noticeable drop in the measured data was caused by an AHU power outage. (see Fig. 5.14 and Fig. 5.15, data drop on day 11. - for approximately two hours)

The conditions during the experiment were as follows; the outside air temperature during the day was $6.5 \sim 16.5°C$, during the night the temperature was: $-2.0 \sim 3.5°C$, the outside air humidity was $25 \sim 87\%$ and the humidity in the room was $11 \sim 31\%$.

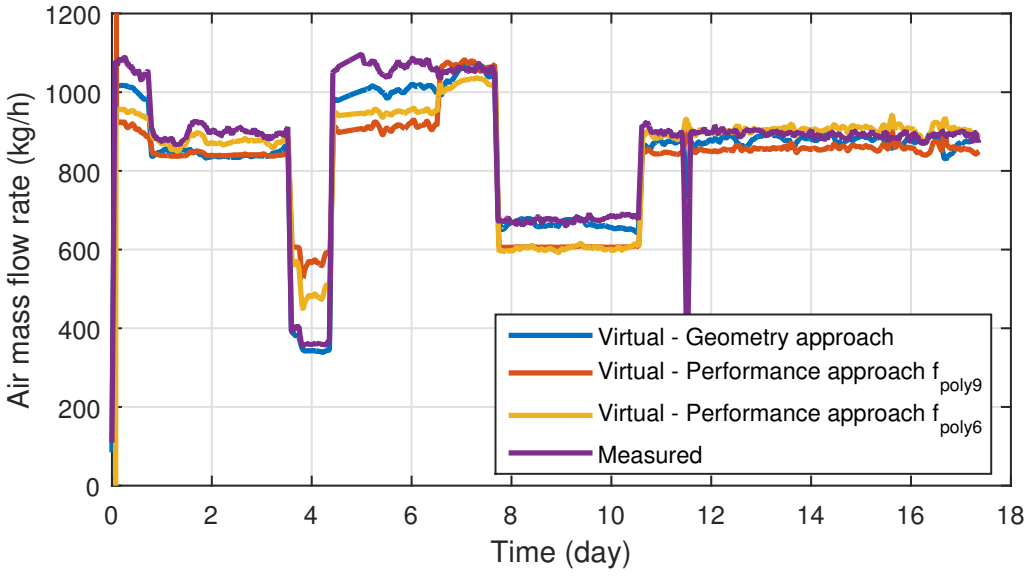

Figure 5.14: Exhaust mass airflows - long-term record

The estimation error (see Table 5.6) is calculated as the relative deviation between the virtual sensor and the physical sensor, which was chosen as the reference data source. In the following, the term 'accuracy' is loosely used as the reciprocal of the estimation error.

Approach	Highest	Average
Exhaust: Performance curve	±57.6%	±10.8%
Exhaust: Geometry	±6.6%	±3.5%
Supply: Performance curve	±76%	±7.3%
Supply: Geometry	±3.4%	±2.2%

Table 5.6: The estimation error of virtual sensors

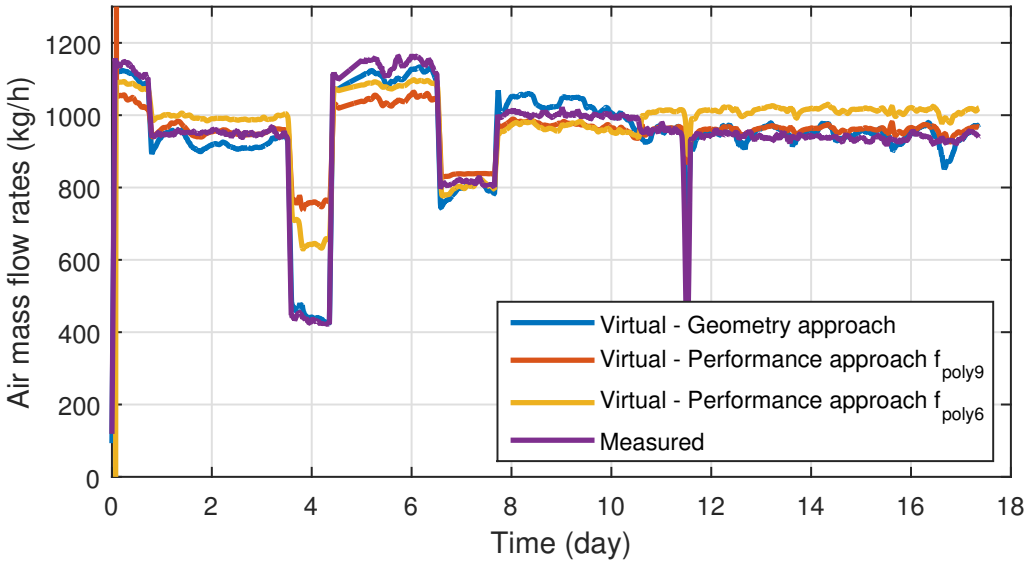

Figure 5.15: Supply mass airflows - long-term record

VS based on a geometry approach provided better results, especially for supply air. The output of VS based on the performance approach also indicates the changes in the air flow, but the values are further from the reference.

The heat exchange process in the recuperator depends on the temperature difference between the two airflows. The temperature difference directly affects the precision of a VS, which is lowest when the difference approaches zero. This phenomenon was observed during the test: the accuracy of the models was reduced at the end of the experiment, after the heating was turned off.

The airflow rates were changed from 400 kg/h to 1100 kg/h with fan speed adjustments. No significant change in the model error correlating with the flow rate was discovered. The models are less precise when the air flows are asymmetrical, especially for exhaust air. This correlation was studied more closely in the experiments described in section 5.3.8.

5.3.8 The use of alternative thermometer positions

In all the experiments, the temperature sensors that provided the values used as inputs to the model were placed in close proximity to the recuperator. This sensor arrangement provides the best results and minimizes the errors in temperature measurements. However, commercial AHUs do not necessarily have the same sensor arrangement. For example, instead of measuring the temperature of the supply air right after the recuperator, a sensor is usually placed only after the heater (or cooler). In addition, the temperature of the

exhaust air before the recuperator often remains unmeasured, and a thermometer inside the ventilated room can be used instead. This placement of the sensors can cause a drop in the accuracy of the flow rate estimation, because the temperatures of the flows are affected by the waste heat from the fans, by imperfections of the heat insulation of the ducts, and by other factors. During the experiments, each measuring point was replaced separately, and then the combination of alternative sensor positions was tested. All the results are demonstrated on the supply air stream (measurement points are numbered according to Fig. 5.5, and Thermometer 11 was placed in the testing chamber).

The experiments with alternative positions of the sensors were performed only for the VS based on the geometric approach.

The VS based on the performance curves approach did not work, due to its high sensitivity to the position of the sensor. Alternative positions of the sensors had a substantial influence on the performance curves model, and caused a high level of deviation from the reference.

Supply air temperature at the inlet of the recuperator

Thermometer number "2" was replaced by thermometer number "1", which measures the outdoor temperature at the very start of the inlet duct.

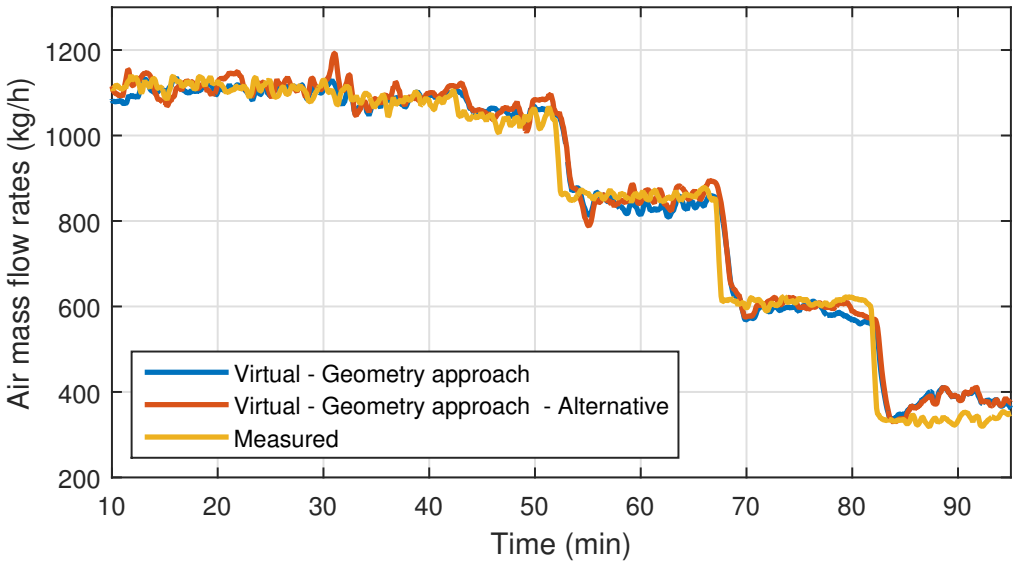

Figure 5.16: Experiment - Thermometer 1

Since there are no significant heat sources between these two sensors, their readings are close to each other. Replacement caused a slight increase in the estimation error, as is shown in Fig. 5.16.

Supply air temperature at the outlet of the recuperator

Thermometer number “3” was replaced by thermometer number “6”, which measures the temperature before the supply air reaches the room at the end of the inlet duct. Since the readings of this sensor were affected by a turned-on heater, the model was unable to estimate the flow rate at all.

Exhaust air temperature at the inlet of the recuperator

Thermometer number "8" was replaced by thermometer number "11", which measures the temperature of the indoor air.

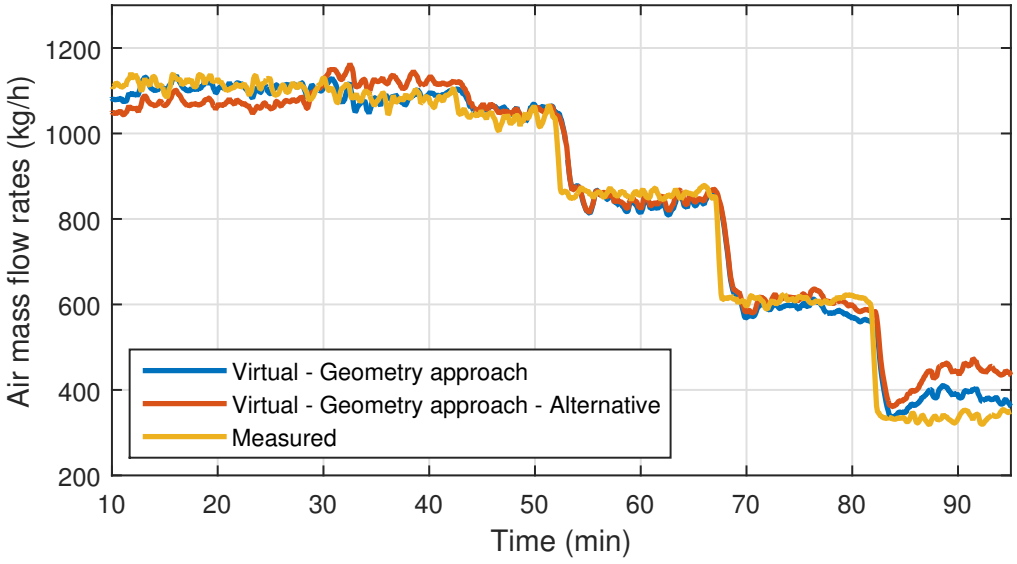

Figure 5.17: Experiment - Thermometer 11

The effect of this replacement on flow rate estimation is stronger than in the case of the Temp 1 sensor, though the changes in supply flow changes can still be recognized (see Fig. 5.17) . The replacement caused an increase in the exhaust air estimation error.

Exhaust air temperature at the outlet of the recuperator

Thermometer number "9" was replaced by thermometer number "10", which measures the temperature of the indoor air at the end of the exhaust duct.

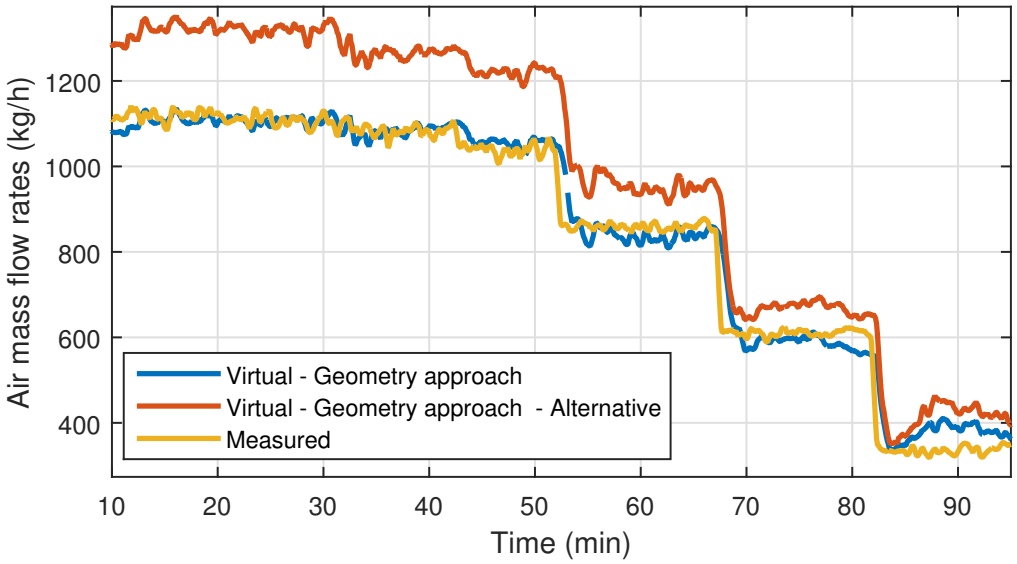

Figure 5.18: Experiment - Thermometer 10

This replacement greatly impacts the estimate of the flow rate. There are significant changes in mass air flow (see Fig. 5.18).

A combination of alternative sensors

The readings from thermometers "2", "8" and "9" were replaced by thermometers "1", "11" and "10", respectively, to examine the simultaneous influence of such replacements.

Although the changes in supply flow are still recognizable (see 5.19), the estimation error may be unacceptable for most applications.

5.4 Discusion

During a number of tests, the mass flow rate of the supply air was estimated with a lower difference from the references than for the flow rate of the exhaust air. This can be explained by the fact that the reference flow meter at the exhaust was placed in close

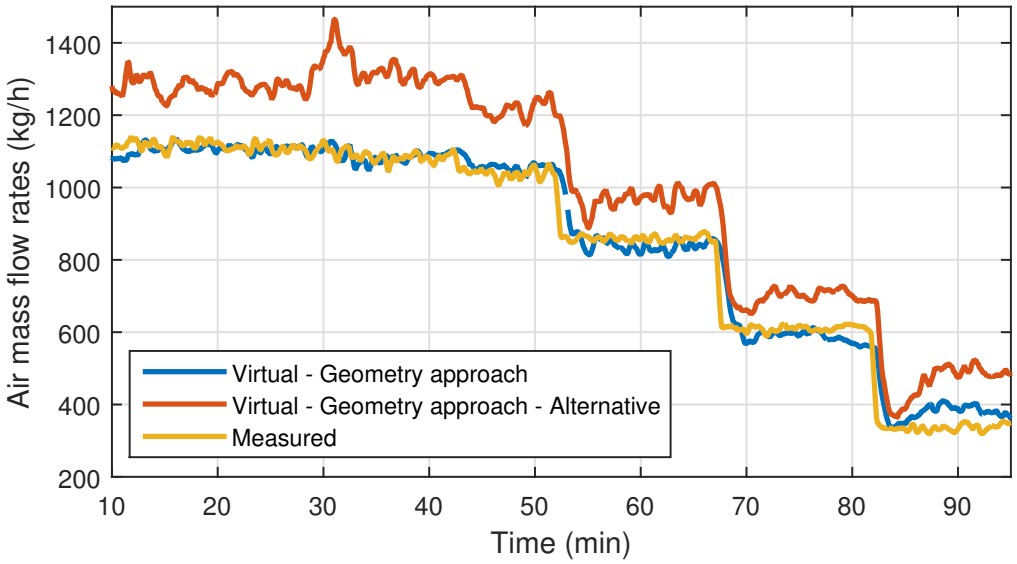

Figure 5.19: Experiment - Thermometers 1, 11 and 10

distance to the duct elbow and was affected by nearby a fan. The fan caused greater disturbances in the reference values, leading to greater inaccuracy of the VS.

The average error of VSs under appropriate conditions was around 10%. VSs are therefore applicable for FDD, but it is necessary to take into account some disadvantages:

- The temperature differences in the denominator of equations 5.2, 5.3, 5.25 and 5.26 have the highest influence on the error of VS. This influence is caused by the temperature measurement accuracy which was $\pm 0.4°C$. The numerical simulations showed that the difference between the outdoor air and the indoor air should be at least $4°C$. When the temperature difference is lower than $4°C$, outputs exceeds the average error of VS. Basically, this means that in moderate climatic conditions VS would have lower accuracy in spring and in autumn.
- Since some simplifications have been made, the method can not guarantee accurate outputs for any type of recuperators without preliminary calibration and validation using a physical flow rate sensor.
- VS models depend on precise temperature measurements: $0.5°C$ or higher error in the temperature measurement leads to a noticeable deviation in the VS readings.

5.5 FDD with virtual mass flow rate sensors

As was previously shown, virtual sensors have certain limitations that reduce their accuracy. According to that, the scenario of partial fault detection and diagnostics methods of AHU units with the virtual air mass flow rate sensor was developed. Geometry or performance curve approach of VS can be used for this FDD algorithm.

FDD Algorithm is intended for short-term diagnostics of the selected AHU unit faults at a time when the thermal comfort can be degraded in the connected zones. The algorithm is described in the figure 5.20. For the best virtual sensor accuracy, AHU unit control is set to an optimal regime for FDD. The obtained mass airflow values can be compared with the values given by the manufacturer or with the values measured in a fault-free state. The condition of the AHU unit can be evaluated based on this comparison. Following faults from the table 2.1 can be detected using FDD algorithm:

- Economizer failure
- Fan malfunction
- Heating / Cooling failure
- Air filter clogging
- Reduced fan efficiency

After the test routine, the original AHU control state can be restored. FDD Algorithm can be evaluated periodically (once a week, month), when the building is not occupied (at night time) or on-demand if AHU unit failure is suspected.

5.6 Conclusions

The proposed virtual air flow rate sensors placed inside an air-conditioning unit have been tested, and the results have indicated that the estimated air flow mass rate values were close to the measured values across the whole range of fan speed.

Typical AHU failures, such as clogged ducts, stuck dampers and damaged fans, could be successfully detected from the VS readings. The characteristic symptom of these failures is reduced mass flow. In a case of difference between estimated mass flow and the set-point of the AHU control system or historical data measured during the faultless operation, the failure can be indicated. Early detection of these failures can prevent unnecessary

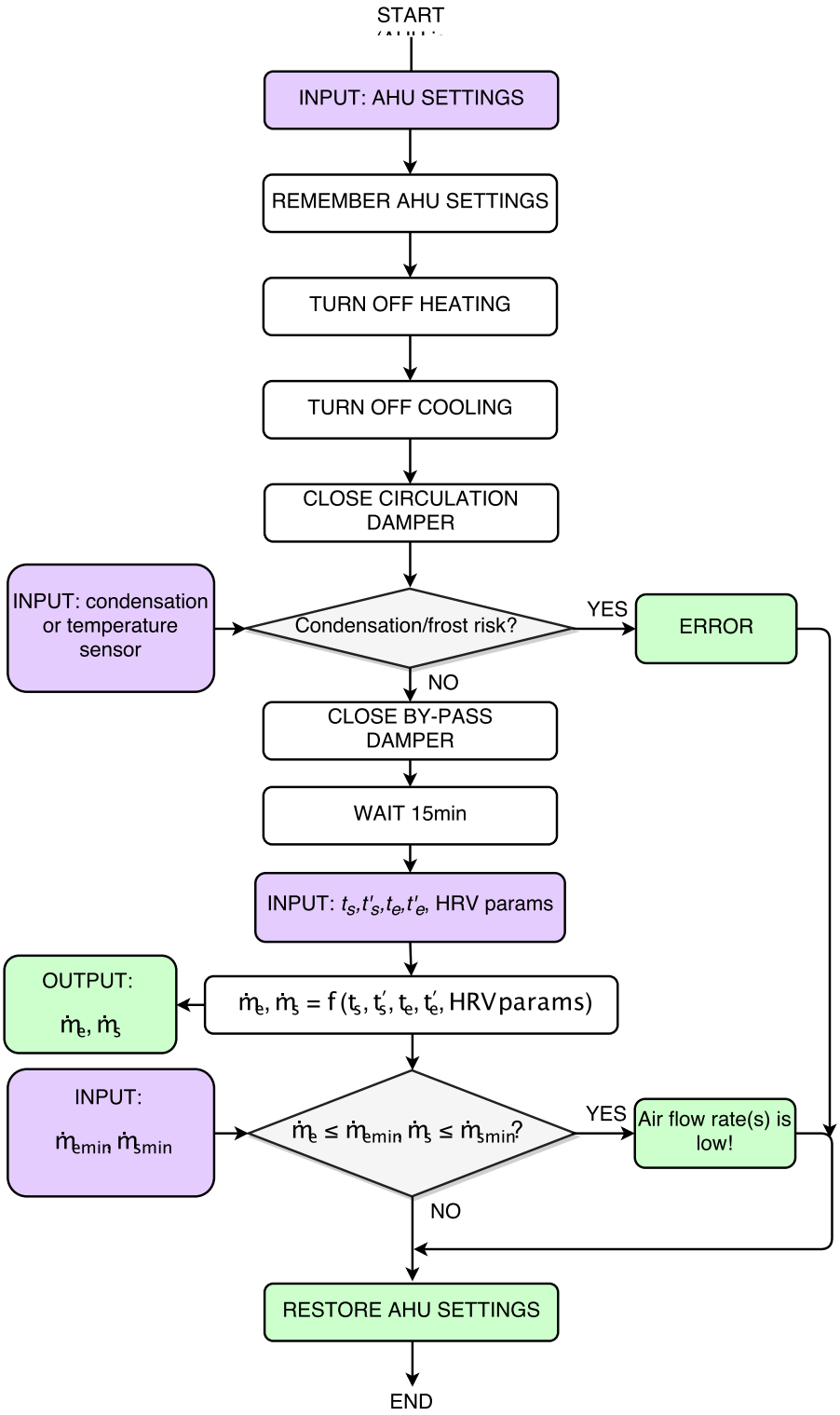

Figure 5.20: State diagram of FDD algorithm

heating/cooling overconsumption, and can as a result decrease the operating cost of a ventilation system.

The parameters of the recuperator needed for the design of a VS can be either in the form of a physical description and a geometrical description of the recuperator, or in the form of the performance curve of the recuperator. Depending on the form in which the recuperator parameters are available, one of the two proposed approaches can be used. The virtual sensor based on the recuperator geometry approach achieved better accuracy than the virtual sensor based on the performance curves approach. However, both approaches achieved an average error of the estimated value of about 10%.

Chapter 6

Conclusion

This thesis is concerned with **virtual sensors and virtual sensing techniques**, for fault detection and diagnostics and data validation. The selected application area is the commercial buildings with the heating, ventilation, and air conditioning system. The thesis has contributed to using the **building information model** for **automatic design and configuration of virtual sensors**. The one advanced method is intended for efficiency check of air handling units base on monitoring of mass flow rate inside the unit. The second developed method is designed for data validation from the zone temperature sensor.

6.1 Recapitulation of this work

The basic ideas of this work are introduced in chapter 1, and the connection between virtual sensors, fault detection and diagnostics methods and building information model is explained. In the section 2.1, an overview of the principles and ideas in virtual sensors are described. Section 2.2 describes the Building Information model, its meaning, and properties. Section 2.2.1 describes ontology, which defines the interface between virtual sensors and building information model. HVAC systems used in commercial buildings, typical faults of HVAC (Heating, Ventilation, and Air Conditioning) systems and fault detection and diagnosis methods using in these systems are described in section 2.3 and 2.4.

A significant challenge for virtual sensors is replacing real sensors that are needed for fault diagnostics. In section 2.4.2, typically missing sensors are identified. Two of these sensors was selected for research, successfully developed and validated in this thesis. A detailed description of these sensors can be found in chapters 4 and 5. Each of these chapters contains a conclusion. Brief description of the results can be found below.

6.2 Contribution of this work

6.2.1 Automated design and configuration of virtual sensors using the building information model

Virtual sensors represent low-cost alternative for missing real sensors. The technical problem that prevents extensive practical use of VS (Virtual Sensors) is their typical demanding configuration for a specific application. **The main goal of this thesis was to prove that the demanding process of virtual sensors configuring can be partially or fully eliminated.** The main objective of the work was divided into two objectives: to develop two types of virtual sensors with automatic configuration using different BIM (Building Information Model) information. **Virtual sensor with automated configuration using information about the geometry and material properties provided by BIM** is summarised in section 6.2.2. **Virtual sensor with an automated parameter setting using information about the HVAC equipment extracted from BIM** is summarised in section 6.2.3. The content of each chapter is summarised, and its main result is put into context with the related chapters.

Configuration of a virtual sensor for a specific application requires a lot of information. As a source of input information, the building information model is used. BIM IFC4.2 standard version 4.2.0.0 specification was selected as ontology for the data interface between BIM and virtual sensors. IFC4.2 contains all entities of the HVAC system, information about building geometry and position, and related parameters. This thesis brings evidence that BIM IFC is a suitable source for automatic configuration of virtual sensors. **Virtual sensors that are published in this thesis can be fully automatically configured using BIM IFC. The objectives described in the chapter 3 are fulfilled.**

This thesis presents possibilities for extension of current fault detection and diagnostics methods in buildings without the need to install new sensors. These methods (algorithm) can be implemented in building control units or systems. The connection to the BIM database must be available. **Using the novel FDD (Fault Detection and Diagnostics) approach, described in this thesis, a reduction in the operating costs of buildings can be reduced**.

For the testing of virtual sensors and fault detection and diagnostics methods, the particular AHU (Air Handling Unit) unit has been developed. Section 5.3.1 describes this unit. AHU unit is connected to one specific testing chamber where various conditions can be set thanks to the possibility to heat or cool each wall separately. A lot of disturbances typical for HVAC units can be simulated.

The results of this thesis have been published in one impact journal [A.1] and presented at several international conferences. Experiment AHU unit has been described and published in Czech periodical [A.8].

6.2.2 Automatically configured virtual sensor using information about the geometry and material properties provided by BIM: Virtual sensor of zone temperature

The virtual sensor, presented in chapter 4, estimates the temperature of the zone based on the information from IFC, temperatures in the surroundings of the zone, and intensity of solar radiation. Information about the building is retrieved from IFC. Geometric information and material properties about windows, doors, ceilings, and walls are extracted. The resulting temperature is estimated using the individual temperature increments across all walls of the zone.

The virtual sensor was tested in a real building. The model output is compared with the real measured temperature in the tested room. The maximum difference between the calculated and the actual temperature is approximately $2°C$. The virtual sensor can be used, for example, to detect a real sensor drift or to detect an open window or door in a room.

6.2.3 Automatically configured virtual sensor using information about the HVAC equipment provided by BIM: Virtual Mass Flow Rate Sensor

The virtual sensor, presented in chapter 5, estimates the mass flow rate inside the AHU unit based on parameters of the recuperator. In this chapter, two virtual mass flow rate sensors are presented. The first VS uses a simplified model of the recuperator, and the second VS uses a performance curve of the recuperator. Parameters of recuperator are automatically obtained from BIM IFC. Example of fault detection and diagnostics method with using of these virtual sensors are described in section 5.5.

The presented virtual sensors placed inside an air-conditioning unit have been tested, and calculated values were close to the measured values across the whole range of fan speed. The virtual sensor based on the recuperator geometry approach achieved better accuracy than the virtual sensor based on the performance curves approach. However, both methods achieved an average error of the estimated value of about 10%. Typical AHU failures, such as clogged ducts, stuck dampers, and damaged fans, could be successfully detected thanks to these VS. Early detection of these failures can decrease the operating cost of a ventilation system.

6.3 Future work

Nowadays, the biggest problem of published methods is the frequent unavailability of the correct and complete information model. Construction and civil engineers do not use

building information models fully; for that reason, some important information is not available in many existing models. BIM quality will gradually improve in the future. There are a lot of important design processes and computations related to HVAC systems, which can be automated based on BIM. Fault detection and diagnostics of the HVAC system is just one of them.

Another area for future work is a detailed uncertainty analysis, which is not covered in this thesis. This analysis is complicated, primarily due to the dynamic nature of the model used for VS and the unavailable uncertainty of the performance curve.

Bibliography

[1] D. Y. Goswami and F. Kreith, *Handbook of Energy Efficiency and Renewable Energy*, CRC Press, 2007, Mechanical engineering series (CRC Press). ISBN 978-0-8493-1730-9.

[2] L. Pérez-Lombard, J. Ortiz, and C. Pout, *A review on buildings energy consumption information*, Energy and Buildings, vol. 40, no. 3, pp. 394–398, 2008.

[3] S. Katipamula and M. R. Brambley, *Review Article: Methods for Fault Detection, Diagnostics, and Prognostics for Building Systems—A Review, Part I*, HVAC&R Research, vol. 11, no. 1, pp. 3–25, 2005.

[4] B. Sučić, A. S. Andelković and Ž. Tomšić, *The concept of an integrated performance monitoring system for promotion of energy awareness in buildings*, Energy and Buildings, 98, 82-91, 2015.

[5] A. Costa, M. M. Keane, J. I. Torrens and E. Corry, *Building operation and energy performance: Monitoring, analysis and optimisation toolkit*, Applied Energy, 101, 310-316, 2013.

[6] M. Gwerder, D. Gyalistras, C. Sagerschnig, R. S. Smith and D. Sturzenegger, *Final Report: Use of Weather and Occupancy Forecasts for Optimal Building Climate Control—Part II: Demonstration (OptiControl-II)*, Automatic Control Laboratory, ETH Zurich: Zug, Switzerland, 156, 2013.

[7] J. Široký, F. Oldewurtel, J. Cigler and S. Prívara, *Experimental analysis of model predictive control for an energy efficient building heating system*, Applied energy, 88(9), 3079-3087, 2011.

[8] S. Katipamula and M. R. Brambley, *Review Article: Methods for Fault Detection, Diagnostics, and Prognostics for Building Systems - A Review, Part II*, HVAC&R Research, vol. 11, no. 2, pp. 169–187, 2005.

[9] Y. Yu, D. Woradechjumroen and D. Yu, *A review of fault detection and diagnosis methodologies on air-handling units*, Energy and Buildings, 82, 550-562, 2014.

[10] H. Li, D. Yu and J. E. Braun, *A review of virtual sensing technology and application in building systems*, HVAC&R Research, vol. 17, no. 5, pp. 619–645, 2011.

[11] H. Li and J. E. Braun, *Economic evaluation of benefits associated with automated fault detection and diagnosis in rooftop air conditioners*, ASHRAE Transactions, 113(2), 200-211, 2007.

[12] V. Venkatasubramanian, R. Rengaswamy, K. Yin and S. N. Kavuri, *A review of process fault detection and diagnosis: Part I: Quantitative model-based methods*, Computers and chemical engineering, 27(3), 293-311, 2003.

[13] J. Trojanova, J. Vass, K. Macek, J. Rojicek and P. Stluka, *Fault Diagnosis of Air Handling Units*, 7th IFAC International Symposium on Fault Detection, Supervision and Safety of Technical Processes, Barcelona, Spain, 2009.

[14] H. Marik, J. Rojicek, P. Stluka and J. Vass, *Advanced HVAC Control: Theory vs. Reality*, Preprints of the 18th IFAC World Congress, Milano (Italy), August 28 - September 2, 2011.

[15] H. Kim, K. Anderson, S. Lee and J. Hildreth, *Generating construction schedules through automatic data extraction using open BIM (building information modeling) technology*, Automation in Construction, vol. 35, pp. 285–295, 2013.

[16] B. Succar, *Building information modelling framework: A research and delivery foundation for industry stakeholders*, Automation in Construction, vol. 18, no. 3, pp. 357–375, 2009.

[17] J. Vass, J. Trojanova, R. Fisera and J. Rojicek, *Embedded Controllers for Increasing HVAC Energy Efficiency by Automated Fault Diagnostics*, 2010.

[18] S. Meyn, A. Surana, Y. Lin, S. M. Oggianu, S. Narayanan and T. A. Frewen, *A sensor-utility-network method for estimation of occupancy in buildings*, in Proceedings of the 48$^{\text{th}}$ IEEE Conference on Decision and Control, 2009 held jointly with the 2009 28$^{\text{th}}$ Chinese Control Conference. CDC/CCC 2009, pp. 1494–1500.

[19] R. Isermann and P. Ballé, *Trends in the application of model-based fault detection and diagnosis of technical processes*, Control Engineering Practice, vol. 5, no. 5, pp. 709–719, 1997.

[20] L. Fortuna, S. Graziani, A. Rizzo and M. G. Xibilia, *Soft Sensors for Monitoring and Control of Industrial Processes*, Springer Science & Business Media, 2007.

[21] W. Yan, H. Shao and X. Wang, *Soft sensing modeling based on support vector machine and Bayesian model selection*, Computers & Chemical Engineering, vol. 28, no. 8, pp. 1489–1498, 2004.

[22] K. Iswandy and A. König, *Hybrid Virtual Sensor Based on RBFN or SVR Compared for an Embedded Application*, in Knowlege-Based and Intelligent Information and Engineering Systems, A. König, A. Dengel, K. Hinkelmann, K. Kise, R. J. Howlett, and L. C. Jain, Eds. Springer Berlin Heidelberg, 2011, pp. 335–344.

[23] F. Heidtmann and D. Soffker, *Virtual Sensors for Diagnosis and Prognosis Purposes in the Context of Elastic Mechanical Structures*, IEEE Sensors Journal, vol. 9, no. 11, pp. 1577–1588, 2009.

[24] A. Bustillo, M. Correa and A. Reñones, *A Virtual Sensor for Online Fault Detection of Multitooth-Tools*, Sensors, vol. 11, no. 3, pp. 2773–2795, 2011.

[25] S. Wang and Y. Chen, *Fault-tolerant control for outdoor ventilation air flow rate in buildings based on neural network*, Building and Environment, vol. 37, no. 7, pp. 691–704, 2002.

[26] M. Ward and J. A. Siegel, *Modeling filter bypass: Impact on filter efficiency. ASHRAE Transactions*, 111(1), 1091-1100, 2005.

[27] G. Y. Jin, W. J. Cai, Y. W. Wang and Y. Yao, *A simple dynamic model of cooling coil unit*, Energy Conversion and Management, vol. 47, no. 15–16, pp. 2659–2672, 2006.

[28] H. Li and J. E. Braun, *A methodology for diagnosing multiple simultaneous faults in vapor-compression air conditioners*, HVACandR Research, 13(2), 369-395, 2007.

[29] B. Tashtoush, M. Molhim and M. Al-Rousan, *Dynamic model of an HVAC system for control analysis*, Energy, vol. 30, no. 10, pp. 1729–1745, 2005.

[30] Handbook, ASHRAE, *Fundamentals*, American Society of Heating, Refrigerating and Air Conditioning Engineers, Atlanta 111, 2001.

[31] K. K. Andersen, H. Madsen and L. H. Hansen, *Modelling the heat dynamics of a building using stochastic differential equations*, Energy and Buildings, vol. 31, no. 1, pp. 13–24, 2000.

[32] S. Karmacharya, G. Putrus, C. Underwood and K. Mahkamov, *Thermal modelling of the building and its HVAC system using Matlab/Simulink*, in 2012 2nd International Symposium on Environment Friendly Energies and Applications (EFEA), 2012, pp. 202–206.

[33] A. J. Smola and B. Schölkopf, *A tutorial on support vector regression*, Statistics and Computing, vol. 14, no. 3, pp. 199–222, 2004.

[34] H. Yang and H. Li, *A Generic Rating-Data-Based (GRDB)DX Coils Modeling Method*, HVAC&R Research, vol. 16, no. 3, pp. 331–353, 2010.

[35] BUILDINGSMART, *International home of omenBIM*, online, 2014, available from: http://www.buildingsmart-tech.org/.

[36] B. Succar, *Building information modelling framework: A research and delivery foundation for industry stakeholders*, Automation in Construction, vol. 18, no. 3, pp. 357–375, 2009.

[37] G. Demchak, T. Dzambazova and E. Krygiel, *Introducing Revit architecture 2009: BIM for beginners*, John Wiley and Sons, (2009).

[38] CEO, NBS and RIBA Enterprises, *NBS National BIM Report 2014*, online, available from: http://www.thenbs.com/topics/bim/articles/nbs-national-bim-report-2014.asp

[39] BUILDINGSMART IFC4, *Industry Foundation Classes IFC4 Official Release*, online, 2014, available from: http://www.buildingsmart-tech.org.

[40] K. U. Ahn, Y. J. Kim, C. S. Park, I. Kim and K. Lee, *BIM interface for full vs. semi-automated building energy simulation*, Energy and Buildings, vol. 68, Part B, pp. 671–678, 2014.

[41] J. O'Donnell, *SIMMODEL: A domain data model for whole building energy simulation*, presented at the IBPSA Conference, 2012.

[42] R. J. Hitchcock and J. Wong, *Transforming IFC architectural view BIMs for energy simulation: 2011*, in Proceedings of Building Simulation 2011, Sydney, 14-16 November.

[43] S. Kota, J. S. Haberl, M. J. Clayton and W. Yan, *Building Information Modeling (BIM)-based daylighting simulation and analysis*, Energy and Buildings, vol. 81, pp. 391–403, 2014.

[44] G. Provan, J. Ploennigs, M. Boubekeur, A. Mady and A. Ahmed, *Using Building Information Model Data for Generating and Updating Diagnostic Models.*

[45] G. Gerauer, O. Rubinova and H. Horka, *Vzduchotechnika: design for efficiency*, Brno, ERA, 2007, xx, 262 s. Mechanical engineering series (Boca Raton, Fla.). ISBN 978-80-7366-091-8.

[46] ASHRAE, *Handbook of HVAC Systems and Equipment*, Atlanta, GA, USA: American Society of Heating, Refrigerating and Air Conditioning Engineers, 2004.

[47] J. F. Kreider, *Heating and cooling of buildings: design for efficiency*, Rev. 2nd ed. Boca Raton: CRC Press/Taylor, c2010, xix, 843 s. Mechanical engineering series (Boca Raton, Fla.). ISBN 978-1-4398-1151-1.

[48] Y. Li, emphElectrical signal based fault detection and diagnosis for rooftop units, ETD collection for University of Nebraska - Lincoln, pp. 1–254, 2012.

[49] M. R. Brambley, N. Fernandez, W. Wang, K. A. Cort, H. Cho, H. Ngo and J. K. Goddard, *Final project report: Self-correcting controls for VAV system faults Filter/Fan/Coil and VAV box sections*, No. PNNL-20452, Pacific Northwest National Lab.(PNNL), Richland, WA (United States), 2011.

[50] S. Li, *A model-based fault detection and diagnostic methodology for secondary HVAC systems*, idea.library.drexel.edu, 2009.

[51] J. Hyvarinen, *Building optimization and fault diagnosis source book*, Technical Research Centre of Finland, VTT Building Technology, 1996, ISBN 95-250-0410-4.

[52] A. S. Glass, P. Gruber, M. Roos and J. Todtli, *Qualitative model-based fault detection in air-handling units*, IEEE Control Systems, vol. 15, no. 4, pp. 11–22, 1995.

[53] S. Katipamula, R. G. Pratt, D. P. Chassin, Z. T. Taylor, K. Gowri and M. R. Brambley, *Automated fault detection and diagnostics for outdoor-air ventilation systems and economizers: Methodology and results from field testing*, ASHRAE Transactions 105(1), 1999.

[54] J. Schein, S. T. Bushby, N. S. Castro and J. M. House, *A rule-based fault detection method for air handling units*, Energy and Buildings, vol. 38, no. 12, pp. 1485–1492, 2006.

[55] J. Schein, *Results from Field Testing of Embedded Air Handling Unit and Variable Air Volume Box Fault Detection Tools*, NISTIR 7365, National Institute of Standards and Technology (NIST), 2006.

[56] N. S. Castro, J. Schein, C. Park, M. A. Galler and S. T. Bushby, *Results from Simulation and Laboratory Testing of Air Handling Unit and Variable Air Volume Box Diagnostic Tools*, 2003.

[57] D. W. Han and Y. S. Chang, *Automated fault diagnosis method for a variable air volume air handling unit*, in ICCAS-SICE, 2009, 2009, pp. 2012–2017.

[58] G. Zimmermann, Y. Lu and G. Lo, *Automatic HVAC fault detection and diagnosis system generation based on heat flow models*, HVAC&R Research, vol. 18, no. 1–2, pp. 112–125, 2012.

[59] J. Ploennigs, A. Ahmed, B. Hensel, P. Stack and K. Menzel, *Virtual sensors for estimation of energy consumption and thermal comfort in buildings with underfloor heating*, Advanced Engineering Informatics, vol. 25, no. 4, pp. 688–698, 2011.

[60] D. Yu, H. Li and M. Yang, *A virtual supply airflow rate meter for rooftop air-conditioning units*, Building and environment, 46(6), 1292-1302, 2011.

[61] F. Kreith and others, *Heat and Mass Transfer Mechanical Engineering Handbook*, Boca Raton: CRC Press LLC, Pages: 46-55, 1999.

[62] W. Zhang, N. Ding, G. Yu and W. Zhou, *Virtual sensors design in vehicle sideslip angle and velocity of the centre of gravity estimation*, In 2009 9th International Conference on Electronic Measurement and Instruments (pp. 3-652). IEEE, 2009.

[63] F. Gustafsson, N. Persson, M. Drevö, U. Forssell, H. Quicklund and M. Löfgren, *Virtual sensors of tire pressure and road friction*, Linköping University Electronic Press, 2001.

[64] H. Li and J. E. Braun, *Decoupling features for diagnosis of reversing and check valve faults in heat pumps*, international journal of refrigeration, 32(2), 316-326, 2009.

[65] A. Bejan and A. D. Kraus, *Heat transfer handbook (Vol. 1)*, John Wiley and Sons, 2003.

[66] D. Yu, H. Li, L. Ni and Y. Yu, *An improved virtual calibration of a supply air temperature sensor in rooftop air conditioning units*, HVACandR Research, 17(5), 798-812, 2011.

[67] H. Cheung and J. E. Braun, *Minimizing data collection for field calibration of steady-state virtual sensors for HVAC equipment*, International Journal of Refrigeration, 69, 96-105, 2016.

[68] P. T. Tsilingiris, *Thermophysical and transport properties of humid air at temperature range between 0 and 100 C*, Energy Conversion and Management, 49(5), 1098-1110, 2008.

[69] D. Moser, *Commissioning Existing Airside Economizer Systems.*, Ashrae journal, 55.3 (2013).

Publications by the Author

[A.1] V. Horyna, O. Hanuš, R. Šmíd, *Virtual Mass Flow Rate Sensor Using a Fixed-Plate Recuperator*. IEEE Sensors Journal. 19(14), 5760-5768. ISSN 1530-437X. DOI 10.1109/JSEN.2019.2894526, 2019.

[A.2] V. Horyna, R. Šmíd, *Virtual Sensors for Diagnostics of Valve*. 10$^{\text{th}}$ International Conference on Condition Monitoring and Machinery Failure Prevention Technologies CM2013/MFPT2013, Krakow, Poland, ISBN 978-1-901892-37-6, 2013.

[A.3] V. Horyna, R. Šmíd, *Virtual Sensors for Machine Condition*. 10$^{\text{th}}$ International Conference on Condition Monitoring and Machinery Failure Prevention Technologies CM2013/MFPT2013, Krakow, Poland, ISBN 978-1-901892-37-6, 2013.

[A.4] V. Horyna, R. Šmíd, *HVAC test bed for research and development of virtual sensors for condition monitoring*. 11$^{\text{th}}$ International Conference on Condition Monitoring and Machinery Failure Prevention Technologies CM2014/MFPT2014, Manchester, UK, ISBN 978-0-903132-57-5, 2014.

[A.5] V. Horyna, P. Makeš, *Automatic extraction of contextual information from building information model for fault detection and diagnosis in buildings*. In POSTER 2014 - 18$^{\text{th}}$ International Student Conference on Electrical Engineering, Czech Technical University, Prague, CZ, ISBN 978-80-01-05499-4, 2014.

[A.6] V. Horyna, O. Hanuš, *Air handling unit test rig for research and development of fault detection and diagnostics methods*. In POSTER 2014 - 18$^{\text{th}}$ International Student Conference on Electrical Engineering, Czech Technical University, Prague, CZ, ISBN 978-80-01-05499-4, 2014.

[A.7] V. Horyna, J. Vass, *Automatické získávání informací o budově z BIM pro moderní řídící algoritmy*. MATUSKA, T., ed. Sympozium Energeticky efektivní budovy 2015. Bustehrad, 2015-10-15. Praha: Společnost pro techniku prostředí, 2015. p. 105-110. 1. vydani. ISBN 978-80-02-02615-0., 2015.

[A.8] O. Hanuš, V. Horyna, D. Adamovský, *Experimentálni vzduchotechnická jednotka pro vývoj a testování virtuálních senzorů a diagnostických metod*. Vytápění, větrání, instalace. 25(2), 66-71. ISSN 1210-1389, 2016.

[A.9] O. Hanuš, V. Horyna, *Virtual Sensor of Mass Flow for Diagnosis of HVAC Unit*. The Twelfth International Conference on Condition Monitoring and Machinery Fail-

ure Prevention Technologies. Oxford, 2015-06-09/2015-06-11. Oxfordshire: Coxmoor Publishing Co., ISBN 978-1-5108-0712-9, 2015.

[A.10] R. Šmíd, V. Horyna, O. Hanuš, *Ontology based automated design of FDD systems*. The Twelfth International Conference on Condition Monitoring and Machinery Failure Prevention Technologies. Oxford, 2015-06-09/2015-06-11. Oxfordshire: Coxmoor Publishing Co., ISBN 978-1-5108-0712-9., 2015.